

Decentralized Contextual Bandits with Network Adaptivity

Chuyun Deng, Huiwen Jia

Department of Industrial Engineering and Operations Research, University of California, Berkeley
{chuyun_deng@berkeley.edu, huiwenj@berkeley.edu}

We consider contextual linear bandits over networks, a class of sequential decision-making problems where learning occurs simultaneously across multiple locations and the reward distributions share structural similarities while also exhibiting local differences. While classical contextual bandits assume either fully centralized data or entirely isolated learners, much remains unexplored in networked environments when information is partially shared. In this paper, we address this gap by developing two network-aware Upper Confidence Bound (UCB) algorithms, NetLinUCB and Net-SGD-UCB, which enable adaptive information sharing guided by dynamically updated network weights. Our approach decompose learning into global and local components and as a result allow agents to benefit from shared structure without full synchronization. Both algorithms incur lighter communication costs compared to a fully centralized setting as agents only share computed summaries regarding the homogeneous features. We establish regret bounds showing that our methods reduce the learning complexity associated with the shared structure from $O(N)$ to sub-linear $O(\sqrt{N})$, where N is the size of the network. The two algorithms reveal complementary strengths: NetLinUCB excels in low-noise regimes with fine-grained heterogeneity, while Net-SGD-UCB is robust to high-dimensional, high-variance contexts. We further demonstrate the effectiveness of our methods across simulated pricing environments compared to standard benchmarks.

Key words: online learning, contextual bandits, distributed learning, federated learning

1. Introduction

Dynamic decision-making over networked systems is central to many real-world applications, including city-level dynamic pricing (e.g., [Qu et al. 2025](#)), distributed recommendation systems (e.g., [Cai et al. 2024](#)), and decentralized resource allocation (e.g., [Asadpour et al. 2020](#)). In this paper, we focus on a contextual multi-armed bandit (MAB) framework motivated by a dynamic pricing problem faced by online on-demand platforms such as Uber and DoorDash. Consider a scenario in which a platform must set prices across multiple locations for the same service (e.g., a ride or food delivery). Each location may exhibit distinct demand patterns. For example, a tourist-heavy city may experience seasonal surges during holidays or festivals, while another may be more sensitive to commuter traffic or local supply constraints. At the same time, cities often share structural factors, such as population density, competitor presence, or event schedules, which influence demand in similar ways. To optimize revenue, the platform needs to learn effective pricing

strategies over time by leveraging both local signals and transferable knowledge across cities. This setting naturally lends itself to a contextual multi-armed bandit (MAB) formulation, which has emerged as a core framework for sequential decision-making in personalized and adaptive environments (Abbasi-yadkori et al. 2011, Li et al. 2010a, Chu et al. 2011, Martínez-Rubio et al. 2019, Mahadik et al. 2020, Jia et al. 2022b).

A straightforward application of contextual MAB to this decision-making problem yields two benchmark approaches. Both formulate each discrete price level as an arm and treat the observed context, including both shared and city-specific features that affect demand, as a whole context. The first constructs an independent contextual MAB for each city, learning pricing strategies based solely on local observations. Although this respects local heterogeneity, it fails to leverage shared structure across cities. The second approach aggregates all data into a single centralized contextual MAB, maximizing information sharing but at the cost of increased communication and a loss of granularity in capturing local demand nuances. We further introduce the details of these two benchmark algorithms in Sections 3.1.

Our goal is to develop algorithms that balance the extremes of fully decentralized and fully centralized learning, enabling effective knowledge transfer across the network while preserving node-level autonomy and minimizing communication overhead. This introduces a new layer of complexity. At the inner layer, we face the classical exploration–exploitation dilemma inherent to online learning, typically measured by cumulative regret. At the outer layer, we must manage a distinct trade-off between communication cost and learning performance: greater communication can accelerate learning and reduce regret, but at the expense of efficiency and scalability. Designing algorithms that capture both levels of trade-off is central to our work.

Recent work has explored various directions to bridge this gap (e.g., Martínez-Rubio et al. 2019, Kolla et al. 2016). However, these approaches either rely on a central server or focus on a non-contextual setting. To address these limitations, we propose a new class of decentralized contextual bandit algorithms that enable principled information sharing across agents through dynamically learned network weights, while preserving local autonomy and operating without a central server. Our approach builds upon and extends previous work by incorporating real-time contextual updates, decentralized gradient-based confidence bounds, and variance-sensitive exploration strategies.

1.1. Related Work

We refrain from surveying the extensive bandit literature and instead focus on three relevant clusters of work.

Upper Confidence Bound Methods. To address the core exploration-exploitation trade-off, two main approaches prevail, UCB-based methods (Chu et al. 2011, Abbasi-yadkori et al. 2011, Garivier and Moulines 2011, Wang et al. 2019, Zhou et al. 2020), which construct optimistic confidence bounds for efficient exploration, and Thompson Sampling (Agrawal and Goyal 2012, 2013, Ferreira et al. 2018, Neu et al. 2022, Xu et al. 2023), which leverages posterior sampling for probabilistic action selection. Beyond these, a growing body of alternative methods has emerged, including information-theoretic (Zhou et al. 2019, Marinov and Zimmert 2021), PAC-based (Li et al. 2022), and neural strategies (Sezener et al. 2020, Zhou et al. 2020, Qi et al. 2024). These methods have been successfully applied to real-world applications and deployed in industrial-scale systems (Li et al. 2010a,b, Durand et al. 2018, Jia et al. 2022a, 2024). In this paper, we propose two UCB-based algorithms achieving sublinear regret on the learning horizon and the network size.

Interactive Bandits. Recent advances in interactive bandits provide promising directions to address this challenge and opportunity arising from richer structure beyond classic bandit settings, including clustering bandits (Korda et al. 2016, Ghosh et al. 2022), multi-task linear bandits (Yang et al. 2021, Hu et al. 2021), and bandits with graph feedback (Wen et al. 2024). Unlike our setting where we consider a network, i.e., graph, over contextual bandit problems, Wen et al. (2024) considers a graph of arms and pulling one arm results in several reward feedback. Szorenyi et al. (2013) combined peer-to-peer communication networks with the ϵ -greedy strategy for distributed multi-armed bandits and Martínez-Rubio et al. (2019) proposed a fully decentralized UCB model to address the classic MAB problem. We adopt the same problem formulation but extend it to the contextual setting. Wang et al. (2020) studied communication-efficient distributed linear bandits where multiple agents interact with a central server by periodically exchanging information, under the assumption that all agents share the same bandit model. Building on this setup, Do et al. (2023) introduced an ϵ -similarity constraint on model parameters to allow for agent-level personalization, while still relying on centralized communication. Similarly, Dubey and Pentland (2020) enhanced privacy through differentially private updates and periodic aggregation, which also retains a centralized architecture. In contrast, our work avoids reliance on a central server and focuses on decentralized real-time updates.

Global and Local Learning. A parallel line of research explores the decomposition of global and local learning. Shi et al. (2021) introduced a combination of global and local exploration with multiple simultaneous pulls and employed trimming techniques to preserve personalization. Huang et al. (2021) developed federated linear bandits that share global parameters while retaining local ones, but their updates are not performed in real time. Li and Wang (2021) followed a similar pattern by jointly estimating global parameters for online learning, achieving an $O(\sqrt{T} \log T)$ regret bound without explicitly designing weights. While their approach relies on global parameter

updates, it does not incorporate fine-grained similarity across agents. Meanwhile, [Kolla et al. \(2016\)](#) studied networked multi-armed bandits, where each node exploits neighbors’ arm-selection patterns to improve decisions. Inspired by this idea, we extend neighborhood collaboration to the contextual linear setting using a fully connected graph, where edge weights reflect both arm-selection frequency and context similarity. Our algorithms leverage this structure to perform real-time updates that balance global sharing with agent-specific learning.

Lastly, we would like to mention two works closely related to our second algorithm, Net-SGD-UCB. [Ba et al. \(2024\)](#) explored doubly optimal learning in monotone games, highlighting the role of gradient sharing in distributed settings. These models strongly motivate our Net-SGD-UCB algorithm, which unifies confidence-based exploration with decentralized gradient aggregation. In addition, [Zhou et al. \(2020\)](#) inspires our design of a novel gradient-based confidence radius, transitioning from the paper’s form $g^\top Gg$ to a context-aware variant $\mathbf{x}^\top G\mathbf{x}$, allowing gradient information to be integrated more directly with contextual structure and supporting decentralized, variance-sensitive exploration.

1.2. Our Contributions

To build a network-aware bandit framework, we develop two online algorithms, NetLinUCB and Net-SGD-UCB, that extend linear contextual bandits to decentralized, multi-agent settings with adaptive information sharing.

- NetLinUCB builds on the classical LinUCB framework ([Li et al. 2010a](#), [Chu et al. 2011](#)) and introduces a neighbor-weighted estimator. Each agent maintains its own local parameters but sequentially incorporates estimates from its neighbors to determine the point estimate and corresponding confidence radius, weighted according to exploration statistics and contextual similarity.
- Net-SGD-UCB applies stochastic gradient descent (SGD) with momentum ([Bottou 2012](#), [Kingma and Ba 2017](#)), combined with adaptive learning rates inspired by AdaGrad ([Duchi et al. 2011](#)). It performs local updates for each agent while incorporating network aggregation to guide learning. This variant is particularly suited to high-dimensional contexts and streaming data scenarios, where memory and computation are limited.

We prove that NetLinUCB achieves $O(\sqrt{\frac{d_c TN}{c}} \log(\frac{cTN}{d_c}) + \sum_{i=1}^N d_{i,s} \sqrt{T \log T})$ regret, where N is the number of nodes, d_c is the shared feature dimension, $d_{i,s}$ is the node-specific feature dimension, and c is a context-diversity constant, defined as a lower bound on the minimum eigenvalue of the empirical context covariance matrix, and it depends on the common feature dimension d_c . Net-SGD-UCB achieves a regret of $O(\frac{\sqrt{Nd_c T \log(\sigma^2 T)}}{1-\gamma} + \sum_{i=1}^N \frac{\sqrt{2d_{i,s} T \log(\sigma^2 T)}}{(1-\gamma)\sigma} + \sigma N \sqrt{\frac{(1-\mu)T \log T}{(1+\mu)(1-\gamma)}})$, where γ is the EMA smoothing factor, μ is the momentum parameter, d_c is the shared feature dimension, $d_{i,s}$ is the node-specific feature dimension, and σ is the variance of noise. We compare the proposed

algorithms with two benchmark models in Section 4.4. In summary, our methods reduce the regret associated with the shared feature space from a linear dependence on the number of nodes $O(N)$ to sublinear $O(\sqrt{N})$, significantly improving sample efficiency.

We validate our models through extensive experiments simulating a distributed pricing system over a network of cities. Both NetLinUCB and Net-SGD-UCB consistently outperform benchmark algorithms, demonstrating faster convergence and significantly lower cumulative regret. The results also reveal several important managerial insights. First, when network connectivity increases, our models exhibit more efficient learning by leveraging information across cities. Second, NetLinUCB is especially effective when reward differences are small, leveraging fine-grained similarity between cities to guide arm selection. Third, Net-SGD-UCB demonstrates strong robustness in the presence of high-variance or noisy contextual features, benefiting from adaptive learning and variance-aware exploration.

1.3. Structure of the Paper

The remainder of this paper is organized as follows. In Section 2, we introduce the decentralized contextual bandit problem and formalize the regret definition under networked decision-making. Section 3 presents the benchmark algorithms (Section 3.1), Disjoint LinUCB and Shared LinUCB, and describes our proposed methods: NetLinUCB (Section 3.3) and Net-SGD-UCB (Section 3.4), which incorporate an adaptive network weight matrix (Section 3.2). In Section 4, we provide theoretical guarantees for all algorithms, including detailed regret bounds and structural insights. Section 5 reports numerical experiments across multiple instances, including convergence rates with respect to time steps T and number of nodes N . In Section 6, we conclude the paper and discuss future research directions. For clarity, all major notation is summarized in Appendix A, and detailed algorithmic steps and proofs are provided in Appendices B through F.

2. Problem Formulation

We consider a network of N nodes. At each node, a decentralized agent is solving a linear contextual MAB instance over T synchronous rounds. The agents share a common problem structure but differ in their local model parameters to capture node-level heterogeneity. At each time step t , the agent at node $i \in [N]$ observes a context vector $\mathbf{x}_{i,t} \in \mathbb{R}^{d_i}$, which consists of a shared component $\mathbf{x}_{i,c,t} \in \mathbb{R}^{d_c}$ and a node-specific component $\mathbf{x}_{i,s,t} \in \mathbb{R}^{d_{i,s}}$, such that $\mathbf{x}_{i,t} = [\mathbf{x}_{i,c,t}, \mathbf{x}_{i,s,t}]$ with $d_i = d_c + d_{i,s}$. The agent then selects an arm $a_{i,t} \in \mathcal{A} = \{a^{(1)}, \dots, a^{(K)}\}$, receives the corresponding reward $r_{i,t}^k$, and updates its local history $\mathcal{D}_{i,t} = \{(\mathbf{x}_{i,\tau}, a_{i,\tau}, r_{i,\tau})\}_{\tau=1}^t$.

For each node i and arm $a^{(k)}$, the reward is modeled as a linear function of the context, $r_{i,t}^k = \mathbf{x}_{i,t}^\top \theta_i^k + \epsilon_{i,t}^k$, where $\epsilon_{i,t}^k \sim \mathcal{N}(0, \sigma_k^2)$ is zero-mean Gaussian noise. The expected reward is therefore

$\mathbb{E}[r_{i,t}^k \mid \mathbf{x}_{i,t}] = \mathbf{x}_{i,t}^\top \theta_i^k$. The linear reward structure is widely adopted in the contextual bandit literature (Li et al. 2010a, Abbasi-yadkori et al. 2011, Dimakopoulou et al. 2018, Wang et al. 2019, Huang et al. 2021, Xu et al. 2023). Each arm $a^{(k)}$ in node i is associated with an unknown coefficient vector, $\theta_i^k = [\theta_c^k, \theta_{i,s}^k] \in \mathbb{R}^{d_i}$, where $\theta_c^k \in \mathbb{R}^{d_c}$ is the shared parameter across all nodes, and $\theta_{i,s}^k \in \mathbb{R}^{d_{i,s}}$ is the node-specific parameter for node i . Under this decomposition, the expected reward for arm $a^{(k)}$ in node i at time t is $\mathbb{E}[r_{i,t}^k \mid \mathbf{x}_{i,t}] = [\mathbf{x}_{i,c}, \mathbf{x}_{i,s}]^\top [\theta_c^k, \theta_{i,s}^k]$.

REMARK 1. Communication Network. In the above setting, we consider a collection of linear contextual bandit problems, where the shared feature space across all nodes has dimension at least one, i.e., $d_c \geq 1$. This condition implies that communication can be helpful between any two nodes. It is equivalent to initializing communication network as fully connected. Importantly, both our proposed algorithms dynamically construct an adaptive weight matrix Ω to guide inter-node information sharing, introduced in Section 3.2. As learning progresses, this mechanism allows the network structure to evolve from fully connected to partially connected or even disjoint structures—based on the informational relevance among agents.

Let $a_{i,t}^*$ denote the optimal arm, $a_{i,t}^* = \arg \max_{k \in \mathcal{A}} \mathbf{x}_{i,t}^\top \theta_i^k$, and $a_{i,t}$ denote the selected arm by the algorithm for node i at time step t . The objective is to maximize cumulative expected reward across all nodes, $\max \mathbb{E}[\sum_t \sum_i r_{i,t}^{a_{i,t}}]$. We adapt the notion of regret and per-trial payoff (e.g., Li et al. 2010a, 2011) as the performance metric. The *instantaneous regret* quantifies the difference between the expected reward of the optimal arm and that of the arm selected by the algorithm at a single time step. The *cumulative regret* aggregates this difference across all trials, measuring the gap between the optimal cumulative reward and the actual cumulative reward.

DEFINITION 1 (CUMULATIVE REGRET). The cumulative regret over the network is defined as

$$R(T) = \mathbb{E} \left[\sum_{t=1}^T \sum_{i=1}^N r_{i,t}^{a_{i,t}^*} \right] - \mathbb{E} \left[\sum_{t=1}^T \sum_{i=1}^N r_{i,t}^{a_{i,t}} \right],$$

where $a_{i,t}^*$ is the optimal arm for node i at time step t , and $a_{i,t}$ is the arm chosen by the algorithm.

ASSUMPTION 1 (Bounded contexts and parameters). *The context vectors $\mathbf{x}_{i,t}$ and arm-specific parameter vectors θ_i^k are bounded such that $\|\mathbf{x}_{i,t}\|_2 \leq 1$, $\|\theta_i^k\|_2 \leq 1$ for all i, k , and t .*

REMARK 2. Assumption 1 is standard in linear bandit analysis. It guarantees that the expected rewards are uniformly bounded, which is essential for applying concentration inequalities and deriving regret bounds. In practice, such boundedness can be achieved via normalization of both features and parameters.

3. Online Algorithms

We present four algorithms in this section, two benchmarks and two newly proposed algorithms. In Section 3.1, we introduce two benchmark algorithms adapted from existing contextual bandits literature and tailored for our setting. In Sections 3.3 and 3.4, we propose two new algorithms specifically designed to facilitate the learning with the consideration of the shared similarities across the network. We derive the theoretical performance guarantee for each of them in Section 4, and then evaluate their numerical performance in Section 5. Both proposed algorithms consider information sharing across the network. Specifically, **NetLinUCB** enables cross-node sharing via adaptive weights, while **Net-SGD-UCB** combines momentum SGD with UCB to enable efficient decentralized learning and adaptive confidence bound construction.

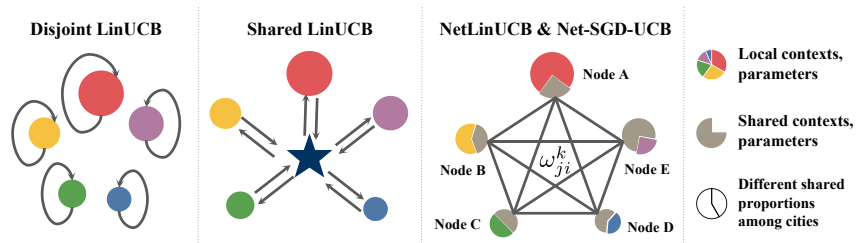


Figure 1 Information sharing structures.

3.1. Benchmark Algorithms

We consider two benchmark algorithms, Disjoint LinUCB and Shared LinUCB, adapted from the well-established contextual bandit literature (Abbasi-yadkori et al. 2011, Chu et al. 2011). Disjoint LinUCB treats each node independently, ignoring any similarities across nodes. In contrast, Shared LinUCB aggregates all data and treats all nodes as a single environment with shared parameters. These two methods represent two extremes in modeling cross-node heterogeneity and serve as natural baselines to evaluate the benefits of network-aware learning.

In **Disjoint LinUCB**, each node $i \in [N]$ maintains an independent LinUCB model and estimates the parameters of all arms with its own local contexts only. At each round, the agent on each node selects the arm that maximizes the upper confidence bound, which is derived based on ridge regression and a context-aware exploration radius. The cumulative regret is $O\left(\sum_{i=1}^N d_i \sqrt{T \log T}\right)$ as established in Theorem 3 of Das and Sinha (2024). We provide detailed algorithmic steps and regret analysis in Appendix B.1 and B.2.

In **Shared LinUCB**, which is a centralized variant, a central agent models all nodes within a unified parameter space by concatenating shared and node-specific features into a global context

vector. For each node, the context corresponds to a distinct sub-block of the global vector, resulting in a block-sparse embedding. Shared LinUCB applies LinUCB over the aggregated context space, yielding a regret bound of $O\left((d_c + \sum_{i=1}^N d_{i,s})\sqrt{T\log T}\right)$, extending the classical result of (Das and Sinha 2024) to a higher-dimensional parameter setting. Detailed algorithmic steps and proofs are deferred to Appendix C.1 and C.2.

Disjoint LinUCB is computationally efficient but lacks information sharing, resulting in slow convergence. Shared LinUCB mitigates this by leveraging shared features, but incurs high computational cost due to its large parameter space. Our proposed algorithms, NetLinUCB and Net-SGD-UCB, address both limitations through structured information exchange and scalable, decentralized estimation. In Section 5, we demonstrate that our models outperform Disjoint LinUCB through cross-agent learning and achieve faster convergence without sacrificing local adaptivity. Moreover, our methods match or exceed the performance of Shared LinUCB while incurring significantly lower computational cost. These improvements highlight the benefits of network-aware estimation and structured exploration in decentralized contextual bandit settings.

3.2. Adaptive Weight Matrix

Benchmark algorithms assume uniform influence across nodes, treating each node independently or equally when aggregating information. In particular, they do not adaptively assign importance to data from different nodes, which may limit performance in the presence of structural heterogeneity.

We first present an essential part of our two newly proposed algorithms, a dynamic weight matrix Ω^k defined for each arm $a^{(k)} \in \mathcal{A}$, which captures evolving similarities between nodes. Each entry $\omega_{ji}^k \in \Omega^k$ quantifies the directional influence from node j to node i . This weight-aware design enables more accurate estimation of shared parameters by prioritizing relevant signals from similar nodes.

We initialize the weight matrix $\Omega^k = I$. As the algorithm proceeds, the weights ω_{ji}^k are dynamically updated over time to reflect evolving similarities between nodes; see Algorithm 1 for the update procedure. Two key components are used to compute a new weight matrix Ω_{new}^k .

- *Arm-selection similarity*, measured by the product $n_j^k n_i^k$, captures how frequently and consistently two nodes select the same arm, indicating stronger mutual relevance.
- *Context similarity*, measured by the cosine similarity between contextual features, assigns higher weights to node pairs with more similar contexts.

After computing these components, all weights are normalized within the network to ensure proper scaling. To ensure computation stability, a smoothing process is applied at every time step, which is

$$\Omega_t^k = \rho \Omega_{t-1}^k + (1 - \rho) \Omega_{\text{new}}^k,$$

where $\rho \in [0, 1)$ is a smoothing coefficient, which controls the influence of newly computed weights relative to historical ones.

Algorithm 1 Weight update

Input: Time step t , arm selection count n_i^k , contexts \mathbf{x} , network \mathcal{G} , smoothing coef ρ .

- 1: **for all** arms $k \in \mathcal{A}$ **do**
- 2: **for all** nodes $i, j \in \mathcal{G}$ **do**
- 3: Compute arm selection similarity: $\frac{n_i^k n_j^k}{(\sum_{q \in \mathcal{G}} n_q^k)^2}$.
- 4: Compute context similarity: $\frac{\mathbf{x}_{i,c}^\top \mathbf{x}_{j,c}}{\|\mathbf{x}_{i,c}\| \cdot \|\mathbf{x}_{j,c}\|}$.
- 5: **end for**
- 6: Combine similarities and normalize to get Ω_{new}^k .
- 7: Update weight matrix: $\Omega^k \leftarrow \rho \Omega_{\text{old}}^k + (1 - \rho) \Omega_{\text{new}}^k$.
- 8: **end for**

Output: Updated weight matrices $\{\Omega^k\}_{k=1}^K$.

3.3. NetLinUCB

To systematically analyze cross-node influences in decentralized contextual bandits, we propose NetLinUCB, a dynamic learning algorithm that incorporates shared contextual effects across nodes via adaptive weighted aggregation. Unlike Disjoint LinUCB, which treats each node independently, and Shared LinUCB, which pools all data globally, NetLinUCB enables partial information sharing while preserving node-level personalization.

Each node decomposes its context into a shared and node-specific part and follows standard ridge regression and UCB-based confidence bounds for local estimation. NetLinUCB then refines these estimates using parameter vectors shared from other nodes, weighted adaptively based on context similarity and arm-selection patterns. The network is assumed to be fully connected, and we investigate how network size affects performance. Arm selection proceeds by maximizing the upper confidence bound as defined in Definition 2, and the complete algorithm is provided in Algorithm 2.

Point estimate. The initial parameter estimates in the Disjoint LinUCB (Appendix B) are obtained via the closed-form solution to ridge regression, $\hat{\theta}_t = (I_d + D_t^\top D_t)^{-1} D_t^\top z_t = W_t^{-1} b_t$, where $W_t = I_d + D_t^\top D_t$ is the design matrix and $b_t = D_t^\top z_t$ is the response vector. Here, $D_t = [\mathbf{x}_\tau^\top]_{\tau \in \Psi_t} \in \mathbb{R}^{|\Psi_t| \times d}$ denotes the context history, $z_t = [r_\tau]_{\tau \in \Psi_t} \in \mathbb{R}^{|\Psi_t| \times 1}$ denotes the reward history, and Ψ_t is the set of time steps prior to t at which arm $a^{(k)}$ was chosen. We further assume that the context vector is ordered such that the first d_c dimensions correspond to the common part, followed by the node-specific part. Consequently, the first d_c coordinates form $W_{i,c}^k$ and $b_{i,c}^k$, while the remaining

$d_{i,s}$ coordinates form $W_{i,s}^k$ and $b_{i,s}^k$. Building on this formulation, NetLinUCB introduces inter-node weighted aggregation to dynamically estimate parameters, i.e.,

$$\hat{\theta}_{i,c}^k = \sum_{j=1}^N \omega_{ji}^k (W_{j,c}^k)^{-1} b_{j,c}^k, \quad \hat{\theta}_{i,s}^k = (W_{i,s}^k)^{-1} b_{i,s}^k,$$

where weight ω_{ji}^k is updated according to Algorithm 1.

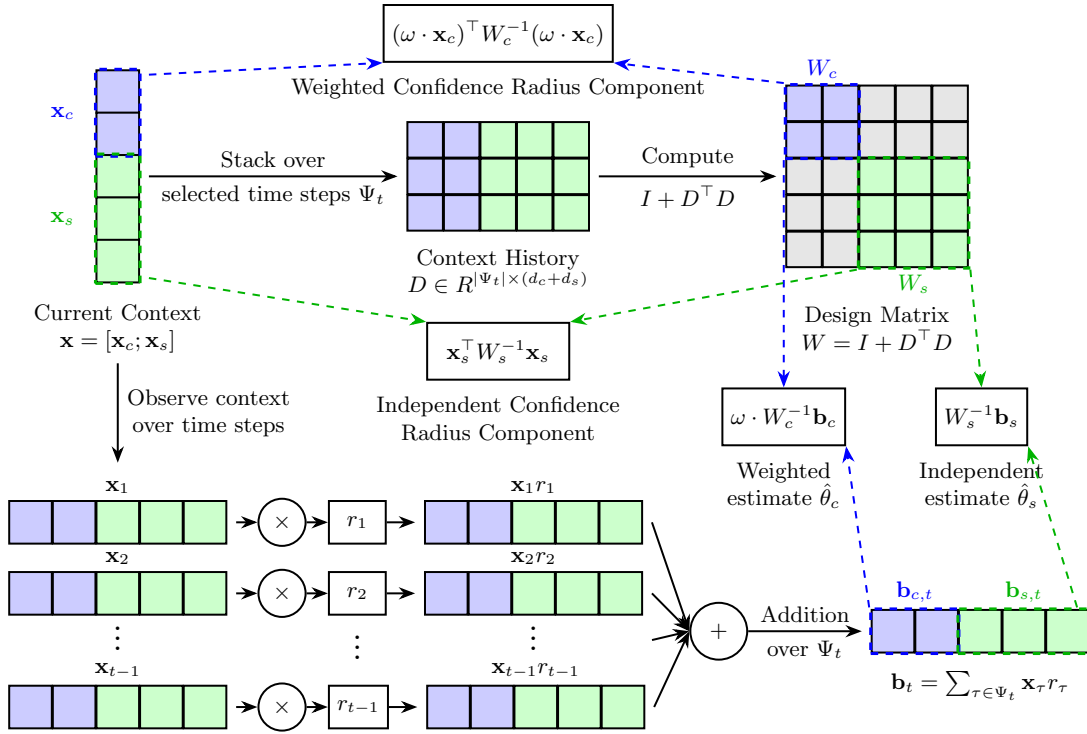


Figure 2 Illustration of NetLinUCB estimation pipeline. The shared and specific context features $\mathbf{x}_{c,t}$, $\mathbf{x}_{s,t}$, and the historical design matrix $D = [D_{c,t}, D_{s,t}]$ are aggregated to form a full design matrix $W = I + D^\top D$. The resulting decomposition yields a weighted estimation of the shared parameter $\hat{\theta}_c$ and a separate estimation of the specific component $\hat{\theta}_s$, with associated confidence radius terms.

Confidence radius. The confidence radius in Disjoint LinUCB is derived from the variance of the historical context, $s_t = \sqrt{\mathbf{x}_t^\top W^{-1} \mathbf{x}_t}$. In NetLinUCB, we decompose W in the same manner as for $\hat{\theta}$, and incorporate other nodes' context histories. The confidence component becomes

$$\sum_{j=1}^N (\omega_{ji}^k)^2 \mathbf{x}_{i,c,t}^\top (W_{j,c}^k)^{-1} \mathbf{x}_{i,c,t},$$

where each weight ω_{ji}^k is squared because the term $(W_{j,c}^k)^{-1}$ represents a variance-level quantity; when aggregating variances, the weights contribute quadratically in contrast to the linear contribution in the point estimates. We also illustrate the estimation pipeline of NetLinUCB in Figure 2.

DEFINITION 2. At each round t , for each arm k and node i , NetLinUCB computes the upper confidence bound as

$$\text{RIDGE-}\mathcal{U}_{i,t}^k = \mathbf{x}_{i,t}^\top [\hat{\theta}_{i,c}^k, \hat{\theta}_{i,s}^k] + \alpha^{\text{ridge}} \cdot \sqrt{\sum_{j=1}^N (\omega_{ji}^k)^2 \mathbf{x}_{i,c,t}^\top (W_{j,c}^k)^{-1} \mathbf{x}_{i,c,t} + \mathbf{x}_{i,s,t}^\top (W_{i,s}^k)^{-1} \mathbf{x}_{i,s,t}},$$

where α^{ridge} is the exploration parameter.

Finally, the arm selection rule integrates both the shared and node-specific estimates along with their corresponding confidence radii, $a_{i,t} = \arg \max_{k \in \mathcal{A}} \text{RIDGE-}\mathcal{U}_{i,t}^k$.

Algorithm 2 NetLinUCB

Input: Number of agents N , arm set \mathcal{A} , context dimension $d_i = d_c + d_{i,s}$, exploration α^{ridge} , network \mathcal{G} .

Parameter: Design matrix $W_i^k \leftarrow I_d$, response vector $b_i^k \leftarrow \mathbf{0}_d$, count matrix $n \leftarrow \mathbf{1} \in \mathbf{Z}_+^{N \times K}$, weight matrix Ω^k for each arm k and node i .

- 1: **for** each round $t = 1$ to T **do**
 - 2: **Update weights** via Algorithm 1.
 - 3: **for all** nodes $i \in \mathcal{G}$ **do**
 - 4: Observe context $\mathbf{x}_{i,t} = [\mathbf{x}_{i,c,t}; \mathbf{x}_{i,s,t}]$.
 - 5: Compute estimates and confidence radii.
 - 6: Select arm $a_{i,t} = \arg \max_{k \in \mathcal{A}} \text{RIDGE-}\mathcal{U}_{i,t}^k$.
 - 7: Observe reward $r_{i,t}$ for the selected arm $k \leftarrow a_{i,t}$.
 - 8: Update n_i^k , W_i^k , and b_i^k .
 - 9: **end for**
 - 10: **end for**
-

3.4. Net-SGD-UCB

To address the scalability challenges of ridge regression with matrix inversion in high-dimensional settings, we propose Net-SGD-UCB. This method replaces closed-form updates with an online Stochastic Gradient Descent with Momentum (SGDM), combined with UCB exploration in a decentralized multi-node setting. Net-SGD-UCB selects the arm with the highest upper confidence bound as defined in Definition 3 and we present the algorithmic details in Algorithm 3.

Point estimate. In classic momentum-based SGD, the gradient is computed using the standard squared loss function $\mathcal{L}_{i,t}^k = \frac{1}{2}(r_{i,t}^k - \hat{r}_{i,t}^k)^2$. After calculating the gradient, parameter estimates $\hat{\theta}$ are sequentially updated using momentum parameter μ and learning rate η^{sgd} as follows.

$$\nabla_{\theta} \mathcal{L}_{i,t}^k = -(r_{i,t}^k - \mathbf{x}_{i,t}^\top \hat{\theta}_{i,t-1}^k) \mathbf{x}_{i,t},$$

$$\begin{aligned}\mathbf{v}_{i,t}^k &= \mu \mathbf{v}_{i,t-1}^k + (1 - \mu) \nabla_{\theta} \mathcal{L}_{i,t}^k, \\ \hat{\theta}_{i,t}^k &= \hat{\theta}_{i,t-1}^k - \eta^{\text{sgd}} \mathbf{v}_{i,t}^k.\end{aligned}$$

Net-SGD-UCB then aggregates information from other nodes with weight matrix Ω^k to form common and node-specific components,

$$\hat{\theta}_{i,c,t}^k = \sum_{j \in \mathcal{G}} \omega_{ji}^k \hat{\theta}_{j,c,t}^k, \quad \hat{\theta}_{i,s,t}^k = \hat{\theta}_{i,s,t}^k,$$

where weight matrix Ω^k is updated based on Algorithm 1.

Confidence radius. In standard SGD-UCB methods, e.g., Zhou et al. (2020), uncertainty is quantified by a geometry term $g^\top G g$, where G accumulates historical gradient information. It captures the observed variation along different parameter directions. To adapt this idea to our context-aware network setting, we maintain only diagonal gradient accumulations. Specifically, we define $G_t = I + \sum_{\tau \in \Psi_t} \nabla_{\theta} \mathcal{L}_{\tau} (\nabla_{\theta} \mathcal{L}_{\tau})^\top$, where Ψ_t denotes the set of time steps before time t when the arm was selected. Because off-diagonal entries add limited value yet increase complexity when combined with the current context, we ignore them and update the diagonal elements,

$$(G_t^k)_{hh} = \gamma (G_{t-1}^k)_{hh} + (1 - \gamma) \left(\frac{\partial \mathcal{L}_t^k}{\partial \theta_h} \right)^2,$$

where $h \in \{1, \dots, d_c + d_s\}$, and $\gamma \in [0, 1)$ is a smoothing parameter that balances historical and recent gradient information. Finally, we partition each diagonal matrix into a common component and a node-specific component, forming $G_{j,c}^k$ and $G_{j,s}^k$, respectively.

DEFINITION 3. At round t , for arm k and node i , Net-SGD-UCB computes the upper confidence bound as

$$\text{SGD-}\mathcal{U}_{i,t}^k = \mathbf{x}_{i,t}^\top [\hat{\theta}_{i,c}^k, \hat{\theta}_{i,s}^k] + \alpha^{\text{sgd}} \cdot \sqrt{\sum_{j=1}^N (\omega_{ji}^k)^2 \mathbf{x}_{i,c,t}^\top (G_{j,c,t}^k)^{-1} \mathbf{x}_{i,c,t} + \mathbf{x}_{i,s,t}^\top (G_{i,s,t}^k)^{-1} \mathbf{x}_{i,s,t}},$$

where α^{sgd} is the exploration parameter and $G_{j,c,t}^k$, $G_{i,s,t}^k$ are EMA-smoothed diagonal gradient matrices.

Finally, the upper confidence bound for arm selection balances exploitation with this adaptive uncertainty. Based on the criterion, we select the arm at time step t as $a_{i,t} = \arg \max_{k \in \mathcal{A}} \text{SGD-}\mathcal{U}_{i,t}^k$.

4. Theoretical Performance Guarantee

In this section, we derive theoretical performance guarantees (Definition 1) for the aforementioned algorithms, two newly proposed algorithms and two adapted benchmark algorithms. In Section 4.4, we further compare them in terms of computational complexity, communication cost, parameter sharing structure, and theoretical regret bounds.

Algorithm 3 Net-SGD-UCB

Input: Number of agents N , arm set \mathcal{A} , context dimension $d_i = d_c + d_{i,s}$, learning rate η^{sgd} , momentum μ , exploration parameter α^{sgd} , EMA smoothing coefficient γ , network \mathcal{G} .

Parameter: Parameter estimates $\hat{\theta}_{i,t}^k$, momentum vectors $\mathbf{v}_{i,t}^k \leftarrow \mathbf{0}$, weight matrix Ω^k , and gradient accumulators $G_{i,t}^k \leftarrow I_d$ for arm k and node i .

- 1: **for** each round $t = 1$ to T **do**
- 2: **Update weights** via Algorithm 1.
- 3: **for all** nodes $i \in \mathcal{G}$ **do**
- 4: Observe context $\mathbf{x}_{i,t} = [\mathbf{x}_{i,c,t}; \mathbf{x}_{i,s,t}]$.
- 5: Compute estimates and confidence radii.
- 6: Select arm $a_{i,t} = \arg \max_{k \in \mathcal{A}} \text{SGD-}\mathcal{U}_{i,t}^k$.
- 7: Observe reward $r_{i,t}$ for the selected arm $k \leftarrow a_{i,t}$.
- 8: Update:

$$\begin{aligned} \nabla_{\theta} \mathcal{L}_{i,t}^k &\leftarrow -(r_{i,t}^k - \mathbf{x}_{i,t}^{\top} \hat{\theta}_{i,t-1}^k) \mathbf{x}_{i,t}, \\ \mathbf{v}_{i,t}^k &\leftarrow \mu \mathbf{v}_{i,t-1}^k + (1 - \mu) \nabla_{\theta} \mathcal{L}_{i,t}^k, \\ \hat{\theta}_{i,t}^k &\leftarrow \hat{\theta}_{i,t-1}^k - \eta^{\text{sgd}} \mathbf{v}_{i,t}^k, \\ G_{i,t}^k &\leftarrow \gamma G_{i,t-1}^k + (1 - \gamma) \text{diag}((\nabla_{\theta} \mathcal{L}_{i,t}^k)^{\odot 2}). \end{aligned}$$

9: **end for**

10: **end for**

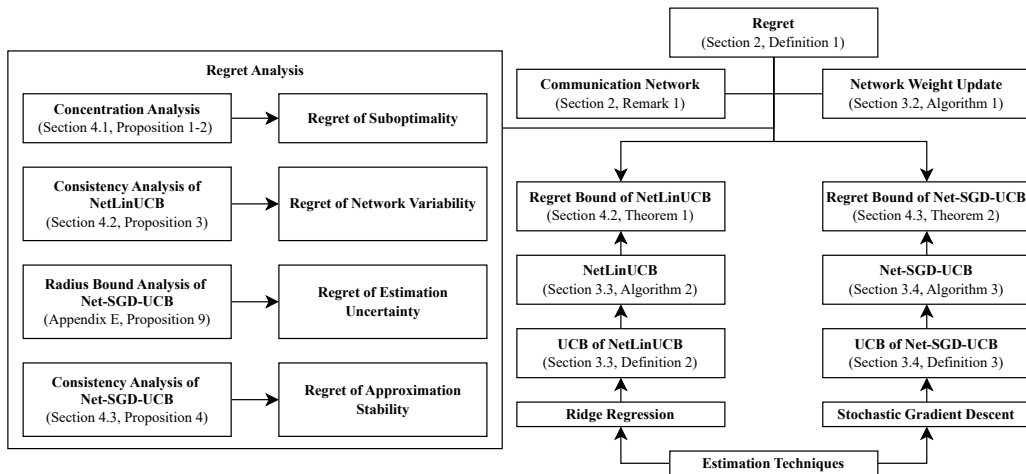


Figure 3 Roadmap of regret analysis.

4.1. Regret Analysis for Benchmarks

We summarize the regret guarantees for the two benchmark algorithms. Specifically, we present their known bounds with respect to the time horizon T and the network size N . We provide detailed proofs in Appendices B and C.

PROPOSITION 1. *The total cumulative regret of Disjoint LinUCB over the network satisfies*

$$R(T) = \sum_{i=1}^N R_i(T) = O\left(\sum_{i=1}^N d_i \sqrt{T \log T}\right).$$

PROPOSITION 2. *The total cumulative regret of Shared LinUCB over the network satisfies*

$$R(T) = O\left(\left(d_c + \sum_{i=1}^N d_{i,s}\right) \sqrt{T \log T}\right).$$

These two benchmark algorithms represent two extremes. Shared LinUCB has a much lower regret by jointly exploiting all contextual information, but its effective dimension increases as $d_c + \sum_i d_s$, resulting in costly matrix operations and high computational burden when the number of nodes N and the context dimensions are large. In contrast, Disjoint LinUCB is computationally efficient with lighter storage and simpler updates, but suffers from higher regret due to the lack of cross-node information sharing. Our goal is to strike a trade-off: achieving a cumulative regret of $\tilde{O}(\sqrt{T})$ while leveraging shared components to approach \sqrt{N} or $\sqrt{d_c}$ scaling, without incurring the full computational burden of the shared model.

4.2. Regret Analysis for NetLinUCB

The overall regret over the network can be naturally decomposed as the sum of the regret of each node in the network. We first provide high-probability bounds for each node and arm in Proposition 3. Then, based on these error bounds, we extend the single-node result to the entire network in Theorem 1, and yield one of the key theoretical results of this paper, the regret bound for NetLinUCB over the network.

We start with a specific node and a specific arm and analyze the confidence radius at time step $t \in [1, T]$. Without loss of generality, we replace the notation $\mathbf{x}_{i,c,t}$ with $\mathbf{x}_{c,t}$, θ_i with θ , $\hat{\theta}_{i,t}$ with $\hat{\theta}_t$, and ω_{ji}^k with ω_j in Proposition 3.

PROPOSITION 3 (**Regret consistency under weighted confidence radius of NetLinUCB**).

At each time step t , given historical information, independent contexts $\{\mathbf{x}_\tau\}_{\tau \in \Psi_t}$ and rewards $\{r_\tau\}_{\tau \in \Psi_t}$, we have

$$\mathbb{P}\left(\left|\mathbf{x}_{c,t}^\top \tilde{\theta}_t - \mathbf{x}_{c,t}^\top \theta\right| \leq (\eta + 1) \tilde{s}_t + \zeta_t\right) \geq 1 - \frac{1}{T}, \quad (1)$$

where $\tilde{\theta}_t = \sum_{j=1}^N \omega_j \hat{\theta}_{j,t}$, $\tilde{s}_t = \sqrt{\sum_{j=1}^N (\omega_j \mathbf{x}_{c,t})^\top W_{j,t}^{-1} (\omega_j \mathbf{x}_{c,t})}$, and ζ_t collects cross-term contributions with $\sum_{t=1}^T \zeta_t = O(1)$. Here, $\eta = \sqrt{\log(2T)}/2$ ensures the stated high-probability guarantee via Hoeffding-type concentration.

We decompose the prediction error into variance and bias terms. The variance is bounded using Azuma's inequality applied to a martingale sum over nodes, while the bias is controlled via the maximal spectral norm of historical context matrices. The full proof is provided in Appendix D.

THEOREM 1 (Cumulative regret of NetLinUCB). *The cumulative regret of the common component in the network is $O\left(\sqrt{\frac{d_c TN}{c} \log\left(\frac{cTN}{d_c}\right)}\right)$, where $c > 0$ is a context-diversity constant, defined as a lower bound on the minimum eigenvalue of the normalized context covariance matrix, and it is related to the common component dimension d_c . The cumulative regret of the node-specific component is $O\left(\sum_{i=1}^N d_{i,s} \sqrt{T \log T}\right)$. Thus, the overall cumulative regret $R(T)$ of the NetLinUCB algorithm is $O\left(\sqrt{\frac{d_c TN}{c} \log\left(\frac{cTN}{d_c}\right)} + \sum_{i=1}^N d_{i,s} \sqrt{T \log T}\right)$.*

Proof sketch of Theorem 1. We split the cumulative regret into shared and node-specific parts.

- For the shared term, Proposition 3 provides a high-probability error bound. We use the lower bound on the minimum eigenvalue of $W_{j,t} = I + \sum_{\tau \in \Psi_{j,t}^k} \mathbf{x}_{j,\tau} \mathbf{x}_{j,\tau}^\top$. The contexts span the feature space and therefore there exists a constant $c > 0$ such that $\lambda_{\min}\left(\frac{1}{|\Psi_{j,t}^k|} \sum_{\tau \in \Psi_{j,t}^k} \mathbf{x}_{j,\tau} \mathbf{x}_{j,\tau}^\top\right) \geq c$, which implies $\mathbf{x}^\top (W_{j,t})^{-1} \mathbf{x} \leq \frac{d_c}{1+c|\Psi_{j,t}^k|}$. Let $n_t^k = \sum_{i=1}^N |\Psi_{j,t}^k|$. Regret terms can then be grouped by the chosen arm k , whenever the arm k is selected $m = 1, \dots, n_T^k$ times, the cumulative contribution behaves as $\sum_{m=1}^{n_T^k} \sqrt{\frac{d_c}{cm}}$, which follows the same summation structure as in classical bandit analysis and is bounded by $O\left(\sqrt{\frac{d_c}{c} n_T^k \log n_T^k}\right)$. Summing over all arms with $\sum_k n_T^k = NT$ yields $O\left(\sqrt{\frac{d_c TN}{c} \log\left(\frac{cTN}{d_c}\right)}\right)$ for the shared part.

- The node-specific part reduces to N disjoint problems, each with regret $O(d_{i,s} \sqrt{T \log T})$.

We provide a full proof in Appendix D.

Q.E.D.

4.3. Regret Analysis for Net-SGD-UCB

The proof roadmap in this section parallels that of NetLinUCB in Section 4.2. We first establish a high-probability regret bound for each node in Proposition 5 and then aggregate the node-level results to obtain the overall regret over the network in Theorem 2. To support Proposition 5, we first derive a SGD-based confidence radius with adaptive weights in Proposition 4, based on an accumulation bound for non-negative sequences in Lemma 1.

LEMMA 1 (Accumulation bound, Duchi et al. (2011), Lemma 4). *Let $\{a_t\}_{t=1}^T$ be a non-negative sequence with cumulative sum $A_t = \sum_{\tau=1}^t a_\tau$. Then, $\sum_{t=1}^T (a_t/A_t) \leq \log(1 + A_T/A_1) + 1$.*

We consider the bound of the constructed confidence radius term for each arm k on a per-node basis. For notational simplicity, we replace the context $\mathbf{x}_{i,t}$ by \mathbf{x}_t , the gradient accumulation matrix $G_{i,t}^k$ by G_t , estimates $\hat{\theta}_{i,t}^k$ by $\hat{\theta}_t$, and the sub-Gaussian noise in the reward function $\epsilon_{i,t}^k$ by ϵ_t .

PROPOSITION 4 (Confidence radius bound). *Under the EMA smoothing scheme and the MSGD setting, where the reward is a linear function with sub-Gaussian noise ϵ , the cumulative term $\sum_t \mathbf{x}_t^\top G^{-1} \mathbf{x}_t$ is bounded as*

$$\mathbf{x}_t^\top G^{-1} \mathbf{x}_t \leq \sum_{t=1}^T \frac{2d \log(\sigma^2 T)}{(1-\gamma)^2 \sigma^2} + \frac{(1-\mu)\sigma^2 \log T}{(1+\mu)(1-\gamma)},$$

where d is the dimension of the contexts, σ^2 is the variance of the noise of our reward function, μ is the momentum parameter, $\gamma \in [0, 1]$ is the smoothing parameter.

Proof sketch of Proposition 4 We analyze the cumulative quadratic form under EMA smoothing. At each step, the diagonal of the gradient-accumulation matrix satisfies $(G_t)_{hh} = (1-\gamma) \sum_{s=1}^t \gamma^{t-s} \epsilon_s^2(\mathbf{x}_s)_h^2 + \gamma^{t-1}$, which effectively smooths the past squared gradients with an exponential kernel. Using this structure, the key term $\sum_{t=1}^T \mathbf{x}_t^\top G_t^{-1} \mathbf{x}_t$ can be decomposed as a sum over coordinates. For each coordinate, Lemma 1 bounds the harmonic sum $\sum_t \frac{\epsilon_t^2(\mathbf{x}_t)_h^2}{\sum_{s=1}^t \epsilon_s^2(\mathbf{x}_s)_h^2}$ by a logarithmic term, leading to a contribution on the order of $\frac{2d \log(\sigma^2 T)}{(1-\gamma)^2 \sigma^2}$. In parallel, we incorporate the effect of momentum updates. The momentum recursion accumulates past gradients as $v_{i,k}^{(t)} = (1-\mu) \sum_{s=1}^t \mu^{t-s-1} \nabla \mathcal{L}^{(s)}$, and a geometric-series argument together with the variance bound for sub-Gaussian noise yields an additional contribution $\frac{(1-\mu)\sigma^2 \log T}{(1+\mu)(1-\gamma)}$.

Adding both parts gives the stated upper bound. A full step-by-step proof, including all intermediate inequalities, is provided in Appendix E.

Once the bound of the constructed confidence radius is obtained, the subsequent proposition demonstrates how this radius leads to consistent regret guarantees, providing a high-probability regret bound for each node.

PROPOSITION 5 (Regret consistency via radius propagation of Net-SGD-UCB). *Under the conditions of Proposition 4, bounded contexts \mathbf{x}_t , and sub-Gaussian noise ϵ_t with variance σ^2 . With a probability of at least $1 - \frac{1}{T}$, the cumulative regret of Net-SGD-UCB in a single node is bounded by*

$$R(T) \leq 2\alpha^{sgd} \left(\frac{\sqrt{2dT \log(\sigma^2 T)}}{(1-\gamma)\sigma} + \sigma \sqrt{\frac{(1-\mu)T \log T}{(1+\mu)(1-\gamma)}} \right),$$

where $\alpha^{sgd} \propto 1 + \sigma^2$ reflects the sensitivity to noise.

By combining the per-node regret guarantees with the inter-node weight update mechanism, we proceed to derive the cumulative regret bound over the entire network.

THEOREM 2 (Cumulative regret bound of Net-SGD-UCB). *In the Net-SGD-UCB framework, the cumulative regret decomposes into a shared and a node-specific component. The shared component scales as $R_1(T) = O\left(\frac{\sqrt{Nd_c T \log(\sigma^2 T)}}{1-\gamma}\right)$. The node-specific regret satisfies $R_2(T) = O\left(\sum_{i=1}^N \frac{\sqrt{2d_{i,s} T \log(\sigma^2 T)}}{(1-\gamma)\sigma} + \sigma N \sqrt{\frac{(1-\mu)T \log T}{(1+\mu)(1-\gamma)}}\right)$.*

Proof sketch of Theorem 2. We decompose the total regret into two parts: the shared regret from estimating the global parameter θ_c , and the node-specific regret associated with estimating local parameters $\theta_{i,s}$.

- For the shared component, we analyze the estimation error dynamics of each node’s shared parameter under weighted neighbor aggregation and stochastic gradient updates. The error consists of variance and bias terms. The bias vanishes since all nodes share the same true parameter θ_c , and the variance term is bounded by standard decentralized SGD analysis with EMA smoothing. As the number of rounds T grows, this variance diminishes. Therefore, the dominant contribution to regret arises from the weighted confidence radius, which we bound accordingly.

- The node-specific component corresponds to running independent SGD-UCB instances in each node. By applying Proposition 5 and summing the regret across all nodes, we obtain the final bound for this part.

Combining both components yields the overall regret bound. The complete derivation is provided in Appendix E. **Q.E.D.**

4.4. Comparisons and Insights

We compare our two proposed algorithms with two benchmark algorithms in Table 1.

Algorithm	NetLinUCB	Net-SGD-UCB	Disjoint LinUCB	Shared LinUCB
Update rule	Weighted ridge	Momentum SGD	Per-node ridge	Global ridge
Computation	$\mathcal{O}(NK(d_c + d_s)^3)$	$\mathcal{O}(NK(d_c + d_s))$	$\mathcal{O}(NK(d_c + d_s)^3)$	$\mathcal{O}(K(d_c + Nd_s)^3)$
Memory	$\mathcal{O}(NK(d_c + d_s)^2)$	$\mathcal{O}(NK(d_c + d_s))$	$\mathcal{O}(NK(d_c + d_s)^2)$	$\mathcal{O}(K(d_c + Nd_s)^2)$
Communication cost	$\mathcal{O}(N^2Kd_c)$	$\mathcal{O}(N^2Kd_c)$	0	$\mathcal{O}(N^2K(d_c + d_s))$
Exploration	Confidence radius	Adaptive covariant	Confidence radius	Confidence radius
Shared parameters	Weight matrix	Weight matrix	None	Full sharing
Best use case	Decentralized	High-dimensional	Static local	Centralized
Regret bound	$\tilde{\mathcal{O}}(\sqrt{(d_c NT)/c}) + Nd_s\sqrt{T}$	$\tilde{\mathcal{O}}(\sqrt{(d_c NT)/(1-\gamma)}) + N\sqrt{(d_s T)/(1-\gamma)}$	$\tilde{\mathcal{O}}(Nd_c\sqrt{T}) + Nd_s\sqrt{T}$	$\tilde{\mathcal{O}}(d_c\sqrt{T}) + Nd_s\sqrt{T}$

Table 1 Comparison of four contextual bandit models in a networked pricing.

The computation and memory costs of Shared LinUCB scale poorly with the global context size, $d_c + Nd_s$, due to the need for full matrix inversion. In contrast, NetLinUCB and Disjoint LinUCB incur only per-node cost. Net-SGD-UCB avoids matrix inversion entirely, yielding the most efficient complexity of $\mathcal{O}(NK(d_c + d_s))$. Even in low-dimensional settings, the per-round runtime of Shared LinUCB remains several times higher than that of the other algorithms.

We also quantify the communication cost per round. Disjoint LinUCB requires no interaction, while NetLinUCB and Net-SGD-UCB exchange only shared parameter estimates, incurring a communication cost of $\mathcal{O}(N^2Kd_c)$ per round across all arms. In contrast, Shared LinUCB synchronizes the full parameter vector, resulting in $\mathcal{O}(N^2K(d_c + d_s))$ communication per round.

NetLinUCB is suitable for decentralized networks because its regret improves with connectivity while preserving node-specific adaptation (Theorem 1). Net-SGD-UCB performs best in high-dimensional or streaming environments due to its low computational complexity with SGD and diagonal variance (Theorem 2). Disjoint LinUCB is effective when agents operate independently and model sizes are small, benefiting from isolated estimation and minimal memory demands (Proposition 1). Shared LinUCB excels in centralized environments with few nodes, where global coordination justifies the increased computational and memory cost (Proposition 2).

Regret bound reveals that Disjoint LinUCB suffers from redundant shared learning, $\tilde{\mathcal{O}}(Nd_c\sqrt{T})$, while Shared LinUCB reduces this to $\tilde{\mathcal{O}}(d_c\sqrt{T})$. NetLinUCB further improves to $\tilde{\mathcal{O}}(\sqrt{NT/c})$ through adaptive network averaging, and Net-SGD-UCB achieves similar gains via variance-aware updates. Both proposed methods better exploit structure for improved regret in decentralized systems. We conducted numerical experiments in Section 5, and the results align with our theoretical insights: models with structured information sharing achieve lower regret and faster convergence rates.

5. Numerical Experiments

We simulate a networked contextual bandit environment with synthetic instances generated as follows. Model parameters θ_i^k are randomly initialized for each node. At each time step t , context vectors are sampled from multivariate Gaussian distributions, with node-specific components drawn from local distributions to reflect heterogeneity. As our interest lies in how regret scales with the learning horizon T and network size N , we report two key metrics: the average per-round regret over time, $R(t)/t$, and the average per-round per-node regret, $R(T)/(NT)$.

Sublinear regret in T . Figure 4 shows the per-round regret over time, $R(t)/t$. As the curves decrease towards zero, the two proposed algorithms achieve sublinear regret in T , matching the centralized benchmark while operating in a decentralized setting. Additional results across multiple instances are provided in Appendix F. Across all instances, network-based models outperform Disjoint LinUCB by effectively leveraging inter-city information. Shared LinUCB performs best when the proportion of shared context is extremely high and the reward gap between the optimal and suboptimal arms is large. This is because (i) a high proportion of shared context induces strong homogeneity across cities, making shared learning highly effective; and (ii) a large arm-reward gap enables the algorithm to quickly identify optimal arms using shared knowledge, thereby accelerating

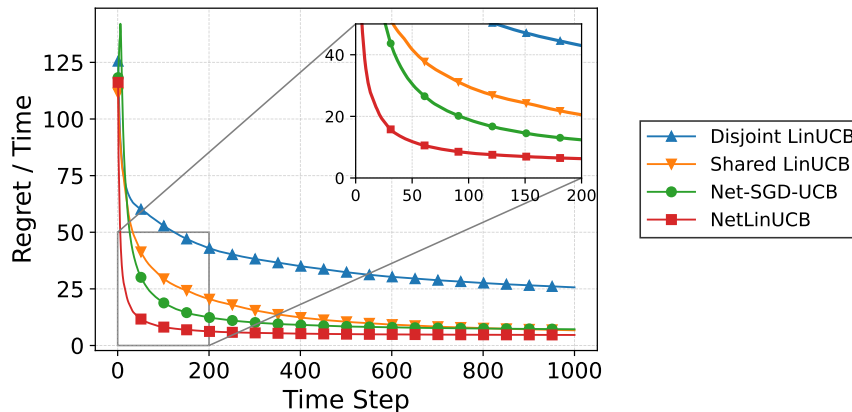


Figure 4 Time-average regret with $T = 1000$ and $N = 12$.

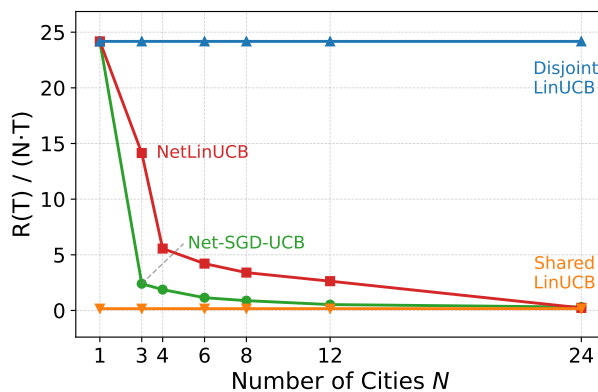


Figure 5 Per-node average regret under different networks.

convergence. Despite its strong empirical performance in these regimes, Shared LinUCB incurs substantially higher per-round computational cost compared to the other methods. NetLinUCB benefits from strong connectivity and performs best when the proportion of node-specific context is extremely high, and arm-reward gaps are small, because it efficiently exploits shared structure to resolve fine-grained differences. Notably, Net-SGD-UCB demonstrates superior robustness in high-variance settings and scales well with larger action spaces due to its adaptive updates.

Sublinear regret on network size N . We present the per-node regret over time $R(t)/(NT)$ of multiple instances in Figure 5. The results show that both NetLinUCB and Net-SGD-UCB achieve a per-node regret as low as the Shared LinUCB, demonstrating sublinear regret scaling in N . This highlights the scalability of network-aware methods in decentralized settings and validates the analysis in Section 3.

6. Conclusion

This work advances decentralized learning for structured decision-making, with broad applications in dynamic pricing, resource allocation, and distributed recommendation systems. We proposed two new UCB-based learning algorithms that achieve sublinear regret and reduce the regret associated with the shared feature space from linear scaling in the number of nodes $O(N)$ to sublinear $O(\sqrt{N})$. A key innovation of our approach lies in its use of adaptive weighting schemes to regulate inter-agent communication, allowing the network to transition between fully connected, partially connected, and even disjoint configurations depending on the agents' informational relevance. Empirically, we demonstrate that increased network connectivity leads to lower regret, validating the benefits of inter-agent information sharing. These findings highlight the potential to improve efficiency in distributed markets while reducing reliance on centralized data, supporting scalability, privacy, and applicability in low-resource settings.

References

- Abbasi-yadkori Y, Pál D, Szepesvári C (2011) Improved Algorithms for Linear Stochastic Bandits. *Advances in Neural Information Processing Systems*, volume 24 (Curran Associates, Inc.), URL https://papers.nips.cc/paper_files/paper/2011/hash/e1d5be1c7f2f456670de3d53c7b54f4a-Abstract.html.
- Agrawal S, Goyal N (2012) Further Optimal Regret Bounds for Thompson Sampling. URL <http://dx.doi.org/10.48550/arXiv.1209.3353>, arXiv:1209.3353 [cs].
- Agrawal S, Goyal N (2013) Thompson Sampling for Contextual Bandits with Linear Payoffs. *Proceedings of the 30th International Conference on Machine Learning*, 127–135 (PMLR), URL <https://proceedings.mlr.press/v28/agrawal13.html>, iSSN: 1938-7228.
- Asadpour A, Wang X, Zhang J (2020) Online resource allocation with limited flexibility. *Management Science* 66(2):642–666.
- Auer P, Cesa-Bianchi N, Fischer P (2002) Finite-time Analysis of the Multiarmed Bandit Problem. *Machine Learning* 47(2):235–256, ISSN 1573-0565, URL <http://dx.doi.org/10.1023/A:1013689704352>.
- Ba W, Lin T, Zhang J, Zhou Z (2024) Doubly Optimal No-Regret Online Learning in Strongly Monotone Games with Bandit Feedback. URL <http://dx.doi.org/10.48550/arXiv.2112.02856>, arXiv:2112.02856 [cs].
- Bottou L (2012) Stochastic Gradient Descent Tricks. Montavon G, Orr GB, Müller KR, eds., *Neural Networks: Tricks of the Trade: Second Edition*, 421–436 (Berlin, Heidelberg: Springer), ISBN 978-3-642-35289-8, URL http://dx.doi.org/10.1007/978-3-642-35289-8_25.
- Cai Q, Cao J, Xu G, Zhu N (2024) Distributed recommendation systems: Survey and research directions. *ACM Transactions on Information Systems* 43(1):1–38.
- Chu W, Li L, Reyzin L, Schapire R (2011) Contextual Bandits with Linear Payoff Functions. *Proceedings of the Fourteenth International Conference on Artificial Intelligence and Statistics*, 208–214 (JMLR Workshop and Conference Proceedings), URL <https://proceedings.mlr.press/v15/chu11a.html>, iSSN: 1938-7228.
- Das N, Sinha G (2024) Linear Contextual Bandits with Hybrid Payoff: Revisited. Bifet A, Davis J, Krilavičius T, Kull M, Ntoutsis E, Žliobaitė I, eds., *Machine Learning and Knowledge Discovery in Databases. Research Track*, 441–455 (Cham: Springer Nature Switzerland), ISBN 978-3-031-70365-2, URL http://dx.doi.org/10.1007/978-3-031-70365-2_26.
- Dimakopoulou M, Zhou Z, Athey S, Imbens G (2018) Estimation Considerations in Contextual Bandits. URL <http://dx.doi.org/10.48550/arXiv.1711.07077>, arXiv:1711.07077 [stat].
- Do A, Nguyen-Tang T, Arora R (2023) Multi-Agent Learning with Heterogeneous Linear Contextual Bandits. *Advances in Neural Information Processing Systems* 36:78768–78790, URL https://proceedings.neurips.cc/paper_files/paper/2023/hash/f8d39584f87944e5dbe46ec76f19e20a-Abstract-Conference.html.
- Dubey A, Pentland A\S (2020) Differentially-Private Federated Linear Bandits. *Advances in Neural Information Processing Systems*, volume 33, 6003–6014 (Curran Associates, Inc.), URL <https://proceedings.neurips.cc/paper/2020/hash/4311359ed4969e8401880e3c1836fbc1-Abstract.html>.
- Duchi J, Hazan E, Singer Y (2011) Adaptive Subgradient Methods for Online Learning and Stochastic Optimization. *Journal of Machine Learning Research* 12(61):2121–2159, ISSN 1533-7928, URL <http://jmlr.org/papers/v12/duchi11a.html>.

- Durand A, Achilleos C, Iacovides D, Strati K, Mitsis GD, Pineau J (2018) Contextual Bandits for Adapting Treatment in a Mouse Model of de Novo Carcinogenesis. *Proceedings of the 3rd Machine Learning for Healthcare Conference*, 67–82 (PMLR), URL <https://proceedings.mlr.press/v85/durand18a.html>, iISSN: 2640-3498.
- Ferreira KJ, Simchi-Levi D, Wang H (2018) Online Network Revenue Management Using Thompson Sampling. *Operations Research* 66(6):1586–1602, ISSN 0030-364X, URL <http://dx.doi.org/10.1287/opre.2018.1755>, publisher: INFORMS.
- Garivier A, Moulines E (2011) On Upper-Confidence Bound Policies for Switching Bandit Problems. Kivinen J, Szepesvári C, Ukkonen E, Zeugmann T, eds., *Algorithmic Learning Theory*, 174–188 (Berlin, Heidelberg: Springer), ISBN 978-3-642-24412-4, URL http://dx.doi.org/10.1007/978-3-642-24412-4_16.
- Ghosh A, Sankararaman A, Ramchandran K (2022) Multi-agent Heterogeneous Stochastic Linear Bandits. *Machine Learning and Knowledge Discovery in Databases: European Conference, ECML PKDD 2022, Grenoble, France, September 19–23, 2022, Proceedings, Part IV*, 300–316 (Berlin, Heidelberg: Springer-Verlag), ISBN 978-3-031-26411-5, URL http://dx.doi.org/10.1007/978-3-031-26412-2_19.
- Hu J, Chen X, Jin C, Li L, Wang L (2021) Near-Optimal Representation Learning for Linear Bandits and Linear RL. *Proceedings of the 38th International Conference on Machine Learning*, 4349–4358 (PMLR), URL <https://proceedings.mlr.press/v139/hu21a.html>, iISSN: 2640-3498.
- Huang R, Wu W, Yang J, Shen C (2021) Federated Linear Contextual Bandits. *Advances in Neural Information Processing Systems*, volume 34, 27057–27068 (Curran Associates, Inc.), URL https://proceedings.neurips.cc/paper_files/paper/2021/hash/e347c51419ffb23ca3fd5050202f9c3d-Abstract.html.
- Jia H, Shi C, Shen S (2022a) Online Learning and Pricing for Network Revenue Management with Reusable Resources. *Advances in Neural Information Processing Systems* 35:4830–4842, URL https://proceedings.neurips.cc/paper_files/paper/2022/hash/1f01cdfd07f0ec78124627cf32d0d83c-Abstract-Conference.html.
- Jia H, Shi C, Shen S (2022b) Online Learning and Pricing with Reusable Resources: Linear Bandits with Sub-Exponential Rewards. *Proceedings of the 39th International Conference on Machine Learning*, 10135–10160 (PMLR), URL <https://proceedings.mlr.press/v162/jia22c.html>, iISSN: 2640-3498.
- Jia H, Shi C, Shen S (2024) Online learning and pricing for service systems with reusable resources. *Operations Research* 72(3):1203–1241.
- Kingma DP, Ba J (2017) Adam: A Method for Stochastic Optimization. URL <http://dx.doi.org/10.48550/arXiv.1412.6980>, arXiv:1412.6980 [cs].
- Kolla RK, Jagannathan K, Gopalan A (2016) Collaborative learning of stochastic bandits over a social network. *2016 54th Annual Allerton Conference on Communication, Control, and Computing (Allerton)*, 1228–1235, URL <http://dx.doi.org/10.1109/ALLERTON.2016.7852375>.
- Korda N, Szorenyi B, Li S (2016) Distributed Clustering of Linear Bandits in Peer to Peer Networks. *Proceedings of The 33rd International Conference on Machine Learning*, 1301–1309 (PMLR), URL <https://proceedings.mlr.press/v48/korda16.html>, iISSN: 1938-7228.
- Li C, Wang H (2021) Asynchronous Upper Confidence Bound Algorithms for Federated Linear Bandits. URL <http://dx.doi.org/10.48550/arXiv.2110.01463>, arXiv:2110.01463 [cs].
- Li L, Chu W, Langford J, Schapire RE (2010a) A Contextual-Bandit Approach to Personalized News Article Recommendation. 661–670, URL <http://dx.doi.org/10.1145/1772690.1772758>, arXiv:1003.0146 [cs].
- Li L, Chu W, Langford J, Wang X (2011) Unbiased Offline Evaluation of Contextual-bandit-based News Article Recommendation Algorithms. 297–306, URL <http://dx.doi.org/10.1145/1935826.1935878>, arXiv:1003.5956 [cs].
- Li W, Wang X, Zhang R, Cui Y, Mao J, Jin R (2010b) Exploitation and exploration in a performance based contextual advertising system. *Proceedings of the 16th ACM SIGKDD international conference on Knowledge discovery and data mining*, 27–36 (Washington DC USA: ACM), URL <http://dx.doi.org/10.1145/1835804.1835811>.
- Li Z, Ratliff L, Nassif H, Jamieson KG, Jain L (2022) Instance-optimal PAC Algorithms for Contextual Bandits. *Advances in Neural Information Processing Systems* 35:37590–37603, URL https://proceedings.neurips.cc/paper_files/paper/2022/hash/f4821075019a058700f6e6738eea1365-Abstract-Conference.html.
- Lian X, Zhang C, Zhang H, Hsieh CJ, Zhang W, Liu J (2017) Can Decentralized Algorithms Outperform Centralized Algorithms? A Case Study for Decentralized Parallel Stochastic Gradient Descent. *Advances in Neural Information Processing Systems*, volume 30 (Curran Associates, Inc.), URL https://proceedings.neurips.cc/paper_files/paper/2017/hash/f75526659f31040afeb61cb7133e4e6d-Abstract.html.
- Mahadik K, Wu Q, Li S, Sabne A (2020) Fast distributed bandits for online recommendation systems. *Proceedings of the 34th ACM International Conference on Supercomputing*, 1–13, ICS '20 (New York, NY, USA: Association for Computing Machinery), ISBN 978-1-4503-7983-0, URL <http://dx.doi.org/10.1145/3392717.3392748>.
- Marinov TV, Zimmert J (2021) The Pareto Frontier of model selection for general Contextual Bandits. *Advances in Neural Information Processing Systems*, volume 34, 17956–17967 (Curran Associates, Inc.), URL https://proceedings.neurips.cc/paper_files/paper/2021/hash/9570efef719d705326f0ff817ef084e6-Abstract.html.
- Martínez-Rubio D, Kanade V, Rebeschini P (2019) Decentralized Cooperative Stochastic Bandits. URL <http://dx.doi.org/10.48550/arXiv.1810.04468>, arXiv:1810.04468 [cs].

- Neu G, Olkhovskaia I, Papini M, Schwartz L (2022) Lifting the Information Ratio: An Information-Theoretic Analysis of Thompson Sampling for Contextual Bandits. *Advances in Neural Information Processing Systems* 35:9486–9498, URL https://proceedings.neurips.cc/paper_files/paper/2022/hash/3d84d9b523e6e82916d496e58761002e-Abstract-Conference.html.
- Qi Y, Ban Y, Banerjee A, He J (2024) Robust Neural Contextual Bandit against Adversarial Corruptions. *Advances in Neural Information Processing Systems* 37:19378–19446, URL https://proceedings.neurips.cc/paper_files/paper/2024/hash/22862040c1781356c8c3df4d00e5811b-Abstract-Conference.html.
- Qu C, Jia H, You P (2025) Decision-dependent distributionally robust optimization with application to dynamic pricing. *arXiv preprint arXiv:2508.06965*.
- Reddi SJ, Kale S, Kumar S (2019) On the Convergence of Adam and Beyond. URL <http://dx.doi.org/10.48550/arXiv.1904.09237>, arXiv:1904.09237 [cs].
- Sezener E, Hutter M, Budden D, Wang J, Veness J (2020) Online Learning in Contextual Bandits using Gated Linear Networks. *Advances in Neural Information Processing Systems*, volume 33, 19467–19477 (Curran Associates, Inc.), URL https://proceedings.neurips.cc/paper_files/paper/2020/hash/e287f0b2e730059c55d97fa92649f4f2-Abstract.html.
- Shi C, Shen C, Yang J (2021) Federated Multi-armed Bandits with Personalization. *Proceedings of The 24th International Conference on Artificial Intelligence and Statistics*, 2917–2925 (PMLR), URL <https://proceedings.mlr.press/v130/shi21c.html>, iISSN: 2640-3498.
- Szorenyi B, Busa-Fekete R, Hegedus I, Ormandi R, Jelasity M, Kegl B (2013) Gossip-based distributed stochastic bandit algorithms. *Proceedings of the 30th International Conference on Machine Learning*, 19–27 (PMLR), URL <https://proceedings.mlr.press/v28/szorenyi13.html>, iISSN: 1938-7228.
- Wang Y, Chen B, Simchi-Levi D (2019) Multi-Modal Dynamic Pricing. URL <http://dx.doi.org/10.2139/ssrn.3489355>.
- Wang Y, Hu J, Chen X, Wang L (2020) Distributed Bandit Learning: Near-Optimal Regret with Efficient Communication. URL https://iclr.cc/virtual_2020/poster_SJxZnR4YvB.html.
- Wen Y, Han Y, Zhou Z (2024) Stochastic contextual bandits with graph feedback: from independence number to MAS number. URL <http://dx.doi.org/10.48550/arXiv.2402.18591>, arXiv:2402.18591 [cs].
- Xu R, Min Y, Wang T (2023) Noise-Adaptive Thompson Sampling for Linear Contextual Bandits. *Advances in Neural Information Processing Systems* 36:23630–23657, URL https://proceedings.neurips.cc/paper_files/paper/2023/hash/4a6824f8f137e78f18e73d9cfc1d22ed-Abstract-Conference.html.
- Yang J, Hu W, Lee JD, Du SS (2021) Impact of Representation Learning in Linear Bandits. URL <http://dx.doi.org/10.48550/arXiv.2010.06531>, arXiv:2010.06531 [cs].
- Zhou D, Li L, Gu Q (2020) Neural Contextual Bandits with UCB-based Exploration. *Proceedings of the 37th International Conference on Machine Learning*, 11492–11502 (PMLR), URL <https://proceedings.mlr.press/v119/zhou20a.html>, iISSN: 2640-3498.
- Zhou Z, Xu R, Blanchet J (2019) Learning in Generalized Linear Contextual Bandits with Stochastic Delays. *Advances in Neural Information Processing Systems*, volume 32 (Curran Associates, Inc.), URL https://papers.nips.cc/paper_files/paper/2019/hash/56cb94cb34617aeadff1e79b53f38354-Abstract.html.

Appendix A: Notation Summary

Notation	Description
$a_{i,t}^{(k)} \in \mathcal{A}$	Arm selected by node i at time t ; index $k = 1, \dots, K$; arm set \mathcal{A}
$b_{i,t}^k$	Response vector in LinUCB parameter update
c	Context diversity constant, lower bound on eigenvalue in LinUCB regret analysis
d, d_i	Context dimension for node i ; $d_i = d_c + d_{i,s}$
d_c	Shared/common context dimension
$d_s, d_{i,s}$	Node-specific context dimension for node i
g	Gradient used in SGD update
h	Index for specific entry of vector or matrix
i, j, q	Indices over nodes
N	Total number of nodes, i.e., $i, j, q \in [N]$
$\mathbf{x}_{i,t}$	Full context vector for node i at time t
$\mathbf{x}_{i,c,t}$	Shared context part for node i at time t
$\mathbf{x}_{i,s,t}$	Node-specific context part for node i at time t
ϵ	Sub-Gaussian noise with zero mean and variance σ^2
r	Reward, modeled as a linear function of context
θ	Model parameters; include shared θ_c and local $\theta_{i,s}$ components
t, τ	Time step indices
\mathbf{v}	Momentum vector in SGD
$G_{i,t}^k$	Diagonal matrix accumulating squared gradients (SGD) for node i , arm k
$W_{i,t}^k$	Design matrix storing historical contexts in LinUCB
s_t	Confidence radius in standard LinUCB, $s_t = \sqrt{\mathbf{x}_t^\top W_t^{-1} \mathbf{x}_t}$
\tilde{s}_t	Weighted confidence radius in NetLinUCB, $\tilde{s}_t = \sqrt{\sum_{j=1}^N (\omega_j \mathbf{x}_{c,t})^\top W_{j,t}^{-1} (\omega_j \mathbf{x}_{c,t})}$
\mathcal{G}	Fully connected network of nodes
Ω^k	Weight matrix for arm k over network \mathcal{G}
ω_{ji}^k	Influence of node j on node i for arm k
γ	EMA smoothing parameter
η	Confidence level parameter in LinUCB regret analysis, $\eta = \sqrt{\frac{1}{2} \log(2T)}$
α^{ridge}	Exploration parameter in NetLinUCB, scaling the confidence radius
α^{sgd}	Exploration parameter in Net-SGD-UCB, scaling the confidence radius
η^{sgd}	Learning rate in SGD update
μ	Momentum coefficient in SGD
$n_{i,t}^k$	Number of times arm k has been selected by node i before time t
n_t^k	Total number of times arm k has been selected by all nodes before time t
$\Psi_{i,t}^k$	Set of time steps before t when arm k was selected; $ \Psi_{i,t}^k = n_{i,t}^k$
$\text{RIDGE-}\mathcal{U}_{i,t}^k$	UCB expression in NetLinUCB using design matrix W
$\text{SGD-}\mathcal{U}_{i,t}^k$	UCB expression in Net-SGD-UCB using gradient-based matrix G

Table 2 Summary of Notation

Appendix B: Supporting Results for Disjoint LinUCB

This section complements the benchmark algorithms presented in Section 3.1. The Disjoint LinUCB algorithm (Chu et al. 2011, Abbasi-yadkori et al. 2011) assumes that, on each node, the coefficients for each arm $a^{(k)}$ are independent, and that context vectors \mathbf{x}_t are shared across all arms.

B.1. Formulation for Disjoint LinUCB

The expected reward of arm $a^{(k)}$ is given by $\mathbb{E}[r_t^k | \mathbf{x}_t] = \mathbf{x}_t^\top \theta^k$. The observed reward of arm $a^{(k)}$ is modeled as $r_t^k = \mathbf{x}_t^\top \theta^k + \epsilon_k$, where θ^k is the true coefficient vector for arm $a^{(k)}$, and $\epsilon_k \sim \mathcal{N}(0, \sigma_k^2)$ is Gaussian noise. At time t , the optimal arm is $a_t^* = \arg \max_{a \in \mathcal{A}} \mathbf{x}_t^\top \theta^a$, while the agent selects $a_t = \arg \max_{a \in \mathcal{A}} \mathbf{x}_t^\top \hat{\theta}^a$ based on estimated parameters. After receiving the corresponding reward, the agent updates its historical data. The cumulative regret over T rounds is defined as $R(T) = \mathbb{E}[\sum_{t=1}^T r_{t,a_t^*}] - \mathbb{E}[\sum_{t=1}^T r_{t,a_t}] = \sum_{t=1}^T \mathbf{x}_t^\top \theta^{a_t^*} - \sum_{t=1}^T \mathbf{x}_t^\top \theta^{a_t}$.

For each arm k , let $s_t = \sqrt{\mathbf{x}_t^\top W_t^{-1} \mathbf{x}_t} \in \mathbb{R}^+$ denote the standard deviation term at round t . Let $D_t = [\mathbf{x}_\tau^\top]_{\tau \in \Psi_t} \in \mathbb{R}^{|\Psi_t| \times d}$ and $z_t = [r_\tau]_{\tau \in \Psi_t} \in \mathbb{R}^{|\Psi_t| \times 1}$ represent the context and reward histories respectively, where Ψ_t is the set of time steps τ when arm k was selected before t . We define the design matrix $W_t = I_d + D_t^\top D_t$ and the response vector $b_t = D_t^\top z_t$. LinUCB uses ridge regression to estimate the coefficient vector via the optimization $\hat{\theta} = \min_{\|\theta\| \leq 1} \|W\theta - b\|^2 + \|I\theta\|^2$, where the regularization parameter is set to $\lambda = 1$. It yields the closed-form solution,

$$\hat{\theta} = (I_d + D_t^\top D_t)^{-1} D_t^\top z_t = W_t^{-1} b_t.$$

LinUCB estimates the reward for each arm by combining the context vector \mathbf{x}_t with the estimated parameter vector $\hat{\theta}_t^k$. To capture uncertainty, it incorporates a confidence term scaled by an exploration parameter α^{ridge} . At each time step, the algorithm selects the arm with the highest upper confidence bound:

$$\hat{r}_t^k = \mathbf{x}_t^\top \hat{\theta}_t^k + \alpha^{\text{ridge}} \sqrt{\mathbf{x}_t^\top W^{-1} \mathbf{x}_t}.$$

This approach balances exploration, selecting arms with greater uncertainty, and exploitation, choosing arms expected to yield higher rewards. LinUCB is computationally efficient and easy to implement, making it well-suited for settings where the linear reward assumption holds.

B.2. Analysis for Disjoint LinUCB

We analyze the regret of the Disjoint LinUCB algorithm following the formulation and results from [Chu et al. \(2011\)](#), [Abbasi-yadkori et al. \(2011\)](#).

PROPOSITION 6 (Error bound for Disjoint LinUCB, [Chu et al. \(2011\)](#), Lemma 1).

Suppose for each node $i \in [N]$, the input index set Ψ_t in Disjoint LinUCB is constructed such that, for any fixed context vector $\mathbf{x}_{i,\tau}$ with $\tau \in \Psi_{i,t}$, the corresponding reward variables $r_{i,\tau}$ are independent random variables with expectations $\mathbb{E}[r_{i,\tau}] = \mathbf{x}_{i,\tau}^\top \theta_i$. Then, with probability at least $1 - \frac{1}{T}$, the following inequality holds uniformly over all arms $a \in \mathcal{A}$ and nodes $i \in [N]$:

$$\left| \mathbf{x}_{i,t}^\top \hat{\theta}_i^a - \mathbf{x}_{i,t}^\top \theta_i^a \right| \leq (\eta + 1) s_{i,t}.$$

Algorithm 4 Disjoint LinUCB

Input: Regularization parameter λ , exploration parameter α^{ridge} , time horizon T .

Parameter: Design matrix $W_k = I_d$, and response vector $b_k = \mathbf{0}_d$ for each arm $k \in \mathcal{A}$.

- 1: **for** $t = 1$ to T **do**
- 2: Observe context $\mathbf{x}_t \in \mathbb{R}^d$.
- 3: **for** each arm $k \in \mathcal{A}$ **do**
- 4: Compute estimate: $\hat{\theta}_t^k \leftarrow W_k^{-1} b_k$.
- 5: Compute UCB: $\hat{r}_t^k \leftarrow \mathbf{x}_t^\top \hat{\theta}_t^k + \alpha^{\text{ridge}} \sqrt{\mathbf{x}_t^\top W_k^{-1} \mathbf{x}_t}$.
- 6: **end for**
- 7: Select arm $a_t = \arg \max_k \hat{r}_t^k$; observe reward r_t .
- 8: Update:

$$\begin{aligned} W_{a_t} &\leftarrow W_{a_t} + \mathbf{x}_t \mathbf{x}_t^\top, \\ b_{a_t} &\leftarrow b_{a_t} + r_t \mathbf{x}_t. \end{aligned}$$

- 9: **end for**

Proof of Proposition 6. Using the standard notation from the Disjoint LinUCB algorithm, we can express the prediction error as

$$\begin{aligned} \mathbf{x}_{i,t}^\top \hat{\theta}_i - \mathbf{x}_{i,t}^\top \theta_i &= \mathbf{x}_{i,t}^\top W_{i,t}^{-1} b_{i,t} - \mathbf{x}_{i,t}^\top W_{i,t}^{-1} (I_d + D_{i,t}^\top D_{i,t}) \theta_i \\ &= \mathbf{x}_{i,t}^\top W_{i,t}^{-1} D_{i,t}^\top r_{i,t} - \mathbf{x}_{i,t}^\top W_{i,t}^{-1} (\theta_i + D_{i,t}^\top D_{i,t} \theta_i) \\ &= \mathbf{x}_{i,t}^\top W_{i,t}^{-1} D_{i,t}^\top (r_{i,t} - D_{i,t} \theta_i) - \mathbf{x}_{i,t}^\top W_{i,t}^{-1} \theta_i. \end{aligned}$$

Because of $\|\theta_i\| \leq 1$ by Assumption 1, we have

$$\left| \mathbf{x}_{i,t}^\top \hat{\theta}_i - \mathbf{x}_{i,t}^\top \theta_i \right| \leq \left| \mathbf{x}_{i,t}^\top W_{i,t}^{-1} D_{i,t}^\top (r_{i,t} - D_{i,t} \theta_i) \right| + \left\| W_{i,t}^{-1} \mathbf{x}_{i,t} \right\|.$$

The right-hand side above decomposes the prediction error into a variance term (first) and a bias term (second). Because the data indexed in $\Psi_{i,t}$ are independent, $E[r_{i,t} - D_{i,t} \theta_i] = 0$. Applying Hoeffding's inequality yields

$$\Pr \left(\left| \mathbf{x}_{i,t}^\top W_{i,t}^{-1} D_{i,t}^\top (r_{i,t} - D_{i,t} \theta_i) \right| > \eta_i s_{i,t} \right) \leq 2 \exp \left(- \frac{2\eta^2 s_{i,t}^2}{\left\| D_{i,t} W_{i,t}^{-1} \mathbf{x}_{i,t} \right\|^2} \right) \leq 2 \exp(-2\eta^2) = \frac{1}{T},$$

where the last inequality follows from the fact that

$$s_{i,t}^2 = \mathbf{x}_{i,t}^\top W_{i,t}^{-1} \mathbf{x}_{i,t} = \mathbf{x}_{i,t}^\top W_{i,t}^{-1} (I_d + D_{i,t}^\top D_{i,t}) W_{i,t}^{-1} \mathbf{x}_{i,t} \geq \mathbf{x}_{i,t}^\top W_{i,t}^{-1} D_{i,t}^\top D_{i,t} W_{i,t}^{-1} \mathbf{x}_{i,t} = (D_{i,t} W_{i,t}^{-1} \mathbf{x}_{i,t})^2.$$

Setting $\eta_i = \sqrt{\frac{\log(2T)}{2}}$ ensures that the tail probability is bounded by $\frac{1}{T}$, i.e.,

$$2 \exp(-2\eta_i^2) = \frac{1}{T}.$$

Applying a union bound over all arms, we can guarantee, with probability at least $1 - 1/T$, that for all arms $a \in \mathcal{A}$,

$$|\mathbf{x}_{i,t}^\top W_{i,t}^{-1} D_{i,t}^\top (r_{i,t} - D_{i,t} \theta_i)| \leq \eta_i s_{i,t}.$$

We now turn to bounding the bias term, where

$$\|W_{i,t}^{-1} \mathbf{x}_{i,t}\| = \sqrt{\mathbf{x}_{i,t}^\top W_{i,t}^{-1} I_d W_{i,t}^{-1} \mathbf{x}_{i,t}} \leq \sqrt{\mathbf{x}_{i,t}^\top W_{i,t}^{-1} (I_d + D_{i,t}^\top D_{i,t}) W_{i,t}^{-1} \mathbf{x}_{i,t}} = s_{i,t}.$$

Combining the variance and bias bounds yields the final result. **Q.E.D.**

PROPOSITION 7 (Determinant-Trace Inequality, Auer et al. (2002), Lemma 11). *Let $\mathbf{x}_1, \mathbf{x}_2, \dots, \mathbf{x}_t \in \mathbb{R}^d$ with $\|\mathbf{x}_\tau\|_2 \leq L$ for all $1 \leq \tau \leq t$, and let $\lambda > 0$. Define $W_t = \lambda I + \sum_{\tau=1}^t \mathbf{x}_\tau \mathbf{x}_\tau^\top$. Then,*

$$\det(W_t) \leq \left(\lambda + \frac{tL^2}{d} \right)^d.$$

Proof of Proposition 7. Let $\lambda_1, \lambda_2, \dots, \lambda_d$ denote the eigenvalues of W_t . Because W_t is symmetric positive definite, all eigenvalues are strictly positive. Note that $\det(W_t) = \prod_{h=1}^d \lambda_h$, and $\text{tr}(W_t) = \sum_{h=1}^d \lambda_h$. By the inequality of arithmetic and geometric means, we have

$$\prod_{h=1}^d \lambda_h \leq \left(\frac{1}{d} \sum_{h=1}^d \lambda_h \right)^d.$$

We now bound the trace,

$$\text{tr}(W_t) = \text{tr}(I) + \sum_{\tau=1}^t \text{tr}(\mathbf{x}_\tau \mathbf{x}_\tau^\top) = d\lambda + \sum_{\tau=1}^t \|\mathbf{x}_\tau\|_2^2 \leq d\lambda + tL^2.$$

Combining the bounds for the determinant and trace, we obtain

$$\det(W_t) \leq \left(\lambda + \frac{tL^2}{d} \right)^d.$$

Q.E.D.

PROPOSITION 8 (Log-Determinant growth, Abbasi-yadkori et al. (2011), Theorem 1).

Let $W_t = \lambda I + \sum_{\tau=1}^t \mathbf{x}_\tau \mathbf{x}_\tau^\top$, then the following inequality holds:

$$\log \left(\frac{\det(W_T)}{\det(W_0)} \right) \leq \sum_{t=1}^T \mathbf{x}_t^\top W_{t-1}^{-1} \mathbf{x}_t.$$

Moreover, if $\|\mathbf{x}_t\|^2 \leq L$ for all t , then

$$\sum_{t=1}^T \min\{1, \mathbf{x}_t^\top W_{t-1}^{-1} \mathbf{x}_t\} \leq 2 \log \left(\frac{\det(W_T)}{\det(W_0)} \right) \leq 2 \left(d \log \left(\lambda + \frac{TL^2}{d} \right) - d \log \lambda \right).$$

Finally, if $\lambda \geq \max(1, L^2)$, then

$$\log \left(\frac{\det(W_T)}{\det(W_0)} \right) \leq \sum_{t=1}^T \mathbf{x}_t^\top W_{t-1}^{-1} \mathbf{x}_t \leq 2 \log \left(\frac{\det(W_T)}{\det(W_0)} \right) \leq 2d \log \left(1 + \frac{TL^2}{d\lambda} \right).$$

Proof of Proposition 8. We first apply the matrix determinant lemma,

$$\det(W_T) = \det(W_{T-1} + \mathbf{x}_t \mathbf{x}_t^\top) = (1 + \mathbf{x}_t^\top W_{T-1}^{-1} \mathbf{x}_t) \det(W_{T-1}).$$

Taking the logarithm on both sides yields

$$\log \det(W_T) = \log(1 + \mathbf{x}_t^\top W_{T-1}^{-1} \mathbf{x}_t) + \log \det(W_{T-1}).$$

Because $\log(1+x) \leq x$ for all $x \geq 0$, we obtain

$$\log \det(W_T) \leq \log \det(W_0) + \sum_{t=1}^T \mathbf{x}_t^\top W_{t-1}^{-1} \mathbf{x}_t.$$

Using the inequality $x \leq 2 \log(1+x)$ for $x \in [0, 1]$, and the previous inequality, we obtain

$$\sum_{t=1}^T \min\{1, \mathbf{x}_t^\top W_{t-1}^{-1} \mathbf{x}_t\} \leq 2 \sum_{t=1}^T \log(1 + \mathbf{x}_t^\top W_{t-1}^{-1} \mathbf{x}_t) = 2 \log \left(\frac{\det(W_T)}{\det(W_0)} \right).$$

To bound the log-determinant ratio, we invoke Proposition 7, which gives

$$\log \det(W_T) \leq d \log \left(\lambda + \frac{TL^2}{d} \right).$$

Because $W_0 = \lambda I$, we have

$$\log \left(\frac{\det(W_T)}{\det(W_0)} \right) \leq d \log \left(\frac{\lambda + \frac{TL^2}{d}}{\lambda} \right) = d \log \left(1 + \frac{TL^2}{d\lambda} \right),$$

finishing the proof of the second inequality.

Lastly, we show that the individual quadratic terms are uniformly bounded if $\frac{L^2}{\lambda} \leq 1$. The sum $\sum_{t=1}^T \mathbf{x}_t^\top W_{t-1}^{-1} \mathbf{x}_t$ can itself be upper bounded as a function of $\log \det(W_T)$ provided that λ is large enough. Using Matrix Inversion proposition, we know

$$\mathbf{x}_t^\top W_{t-1}^{-1} \mathbf{x}_t \leq \frac{\|\mathbf{x}_t\|^2}{\lambda} \leq \frac{L^2}{\lambda}.$$

Hence, we get that if $\lambda \geq \max(1, L^2)$,

$$\log \left(\frac{\det(W_T)}{\det(W_0)} \right) \leq \sum_{t=1}^T \mathbf{x}_t^\top W_{t-1}^{-1} \mathbf{x}_t \leq 2 \log \left(\frac{\det(W_T)}{\det(W_0)} \right) \leq 2d \log \left(1 + \frac{TL^2}{d\lambda} \right).$$

Q.E.D.

By gathering the technical analysis developed in the above propositions, we derive the regret bound for the N -node Disjoint LinUCB algorithm stated in the main text. Below we provide a concise proof sketch.

Proof sketch of Proposition 1. The proof proceeds by summing per-node regret bounds across all N nodes. For each node i , we apply:

- (i) the high-probability prediction error bound from Proposition 6, using a unified confidence parameter η_i ,
- (ii) the determinant-trace bound from Proposition 7 to control the growth of the local design matrix $W_{i,t}$,
- (iii) the cumulative variance bound from Proposition 8:

$$\sum_{t=1}^T \mathbf{x}_{i,t}^\top W_{i,t}^{-1} \mathbf{x}_{i,t} \leq 2d_i \log \left(1 + \frac{T}{\lambda d_i} \right).$$

Using the Cauchy–Schwarz inequality, the per-node regret can be bounded as $R_i(T) = \sum_{t=1}^T \left(\mathbf{x}_{i,t}^\top \theta_i^{a_t^*} - \mathbf{x}_{i,t}^\top \theta_i^{a_t} \right) \leq (1 + \eta_i) \sqrt{T \cdot \sum_{t=1}^T \mathbf{x}_{i,t}^\top W_{i,t}^{-1} \mathbf{x}_{i,t}} = O(d_i \sqrt{T \log T})$. Summing over all nodes gives the network-level cumulative regret:

$$R(T) = \sum_{i=1}^N R_i(T) = O \left(\sum_{i=1}^N d_i \sqrt{T \log T} \right),$$

as claimed. **Q.E.D.**

REMARK 3. This result confirms that LinUCB achieves sub-linear regret in T for each node, ensuring that the algorithm effectively balances exploration and exploitation through the decision-making process.

Appendix C: Supporting Results for Shared LinUCB

This section supplements the benchmark algorithms described in Section 3.1. To capture inter-node dependencies, we adopt a unified framework that embeds both shared and node-specific features within a global parameter space, treating all nodes within a single Disjoint LinUCB model. The shared parameters θ_c^k are initialized uniformly across all nodes, ensuring that they consistently reflect shared contextual influences. As a result, this formulation enhances predictive power and coherence across nodes.

C.1. Formulation for Shared LinUCB

We define a unified feature space of dimension $d = d_c + \sum_{i=1}^N d_{i,s}$, where d_c corresponds to the shared feature dimension and $d_{i,s}$ denotes local features dimension of node i . Each context vector is embedded as $\mathbf{x}_t = [\mathbf{x}_c, \mathbf{x}_{1,s}, \dots, \mathbf{x}_{N,s}] \in \mathbb{R}^d$, and arm-specific parameters are organized as $\theta^k =$

$[\theta_c^k, \theta_{1,s}^k, \dots, \theta_{N,s}^k]$. For node i , only the corresponding shared and local features are active, the expected reward is computed as

$$\mathbb{E}[r_{i,t}^k \mid \mathbf{x}_{i,t}] = [\mathbf{x}_{i,c}, 0, \dots, 0, \mathbf{x}_{i,s}, 0, \dots, 0]^\top \theta^k,$$

where the zero blocks deactivate irrelevant node features.

Algorithm 5 Shared LinUCB

Input: Regularization parameter λ , exploration parameter α^{ridge} , number of nodes N , number of arms K , total dimension $d = d_c + \sum_{i=1}^N d_{i,s}$, time horizon T .

Parameter: Design matrix $W_k = I_d \in \mathbb{R}^{d \times d}$ and response vector $b_k = \mathbf{0}_d \in \mathbb{R}^d$ for each arm k .

- 1: **for** each time step $t = 1$ to T **do**
- 2: **for** each node $i = 1$ to N **do**
- 3: Construct global context vector $\mathbf{x}_{i,t} \in \mathbb{R}^d$: $\mathbf{x}_{i,t} = [\mathbf{x}_{c,t}, 0, \dots, 0, \mathbf{x}_{i,s,t}, 0, \dots, 0]^\top$.
- 4: Compute estimated parameter: $\hat{\theta}_k \leftarrow W_k^{-1} b_k$ for each arm k .
- 5: Select arm $a_{i,t} = \arg \max_k \mathbf{x}_{i,t}^\top \hat{\theta}_k + \alpha^{\text{ridge}} \cdot \sqrt{\mathbf{x}_{i,t}^\top W_k^{-1} \mathbf{x}_{i,t}}$; observe reward $r_{i,t}$.
- 6: Update:

$$\begin{aligned} W_{a_{i,t}} &\leftarrow W_{a_{i,t}} + \mathbf{x}_{i,t} \mathbf{x}_{i,t}^\top, \\ b_{a_{i,t}} &\leftarrow b_{a_{i,t}} + r_{i,t} \cdot \mathbf{x}_{i,t}. \end{aligned}$$

- 7: **end for**
 - 8: **end for**
-

C.2. Analysis for Shared LinUCB

Shared LinUCB can be viewed as a variant of Disjoint LinUCB that aggregates all nodes into a single multi-armed bandit model. Below, we present a concise proof sketch of the regret bound for Shared LinUCB (Proposition 2).

Proof sketch of Proposition 2. We interpret Shared LinUCB as a generalization of Disjoint LinUCB, operating in a higher-dimensional feature space. The cumulative regret is defined as

$$R(T) = \sum_{i=1}^N \sum_{t=1}^T r_{t,a_{i,t}^*} - \sum_{i=1}^N \sum_{t=1}^T r_{t,a_{i,t}}.$$

Using the standard UCB analysis and applying the prediction error bound from Proposition 6, the regret can be bounded by

$$R(T) \leq (1 + \eta) \sum_{t=1}^T \sqrt{\left[\sum_{i=1}^N \mathbf{x}_{i,c,t}, \mathbf{x}_{1,s,t}, \dots, \mathbf{x}_{N,s,t} \right]^\top W_t^{-1} \left[\sum_{i=1}^N \mathbf{x}_{i,c,t}, \mathbf{x}_{1,s,t}, \dots, \mathbf{x}_{N,s,t} \right]}.$$

Applying the log-determinant bound from Proposition 8, we obtain the final regret bound:

$$R(T) = O\left(\left(d_c + \sum_{i=1}^N d_{i,s}\right) \sqrt{T \log T}\right).$$

Q.E.D.

REMARK 4. Shared LinUCB leverages shared and local features via a block-sparse context representation, reducing regret. However, its enlarged parameter space leads to high computational cost, motivating the development of more scalable alternatives such as NetLinUCB and SGD-UCB.

Appendix D: Supporting Results for NetLinUCB

In this section, we derive the weighted confidence radius used in NetLinUCB, building on the core ideas from Disjoint LinUCB. We begin by analyzing the error bound for a specific arm and node, focusing on the shared component of the model. We then generalize the result to include all nodes and arms, ultimately leading to a cumulative regret bound for the entire algorithm.

To motivate the structure of the weighted confidence radius, we adopt the notation and analytical approach of Disjoint LinUCB, adapting it to the multi-node setting with shared parameters; in particular, we focus on analyzing the shared component.

PROPOSITION 9 (**Common component error bound**). *At each time step t , for a given arm, we estimate the parameters and construct a confidence radius based on the accumulated historical information, namely the contexts $\{\mathbf{x}_\tau\}_{\tau \in \Psi_t}$ and observed reward $\{\mathbb{R}_\tau\}_{\tau \in \Psi_t}$. Focusing on the common context component, denoted by $\mathbf{x}_{c,t} = [\mathbf{x}_{c,t}^0, \mathbf{0}]$, we obtain the following bound $\left| \mathbf{x}_{c,t}^\top \hat{\theta}^a - \mathbf{x}_{c,t}^\top \theta^a \right| \leq (\eta + 1)s_t$, which holds with probability at least $1 - \frac{1}{T}$, where $\hat{\theta}^a = W_t^{-1}b_t$ and $s_t = \sqrt{\mathbf{x}_{c,t}^\top W_t^{-1} \mathbf{x}_{c,t}}$.*

Proof of Proposition 9. Using notation consistent with Disjoint LinUCB, we have

$$\begin{aligned} \mathbf{x}_{c,t}^\top \hat{\theta}^a - \mathbf{x}_{c,t}^\top \theta^a &= \mathbf{x}_{c,t}^\top W_t^{-1} b_t - \mathbf{x}_{c,t}^\top W_t^{-1} (I_d + D_t^\top D_t) \theta^a \\ &= \mathbf{x}_{c,t}^\top W_t^{-1} D_t^\top r_t - \mathbf{x}_{c,t}^\top W_t^{-1} (\theta^a + D_t^\top D_t \theta^a) \\ &= \mathbf{x}_{c,t}^\top W_t^{-1} D_t^\top (r_t - D_t \theta^a) - \mathbf{x}_{c,t}^\top W_t^{-1} \theta^a. \end{aligned}$$

Because of $\|\theta^a\| \leq 1$ under Assumption 1, we can bound:

$$\left| \mathbf{x}_{c,t}^\top \hat{\theta}^a - \mathbf{x}_{c,t}^\top \theta^a \right| \leq \left| \mathbf{x}_{c,t}^\top W_t^{-1} D_t^\top (r_t - D_t \theta^a) \right| + \left\| W_t^{-1} \mathbf{x}_{c,t} \right\|.$$

The right-hand side above decomposes the prediction error into two components: a variance term and a bias term. We analyze these two terms separately.

Given the statistical independence of samples indexed in Ψ_t and bounded rewards, we apply Hoeffding's inequality to the variance term,

$$\Pr(|\mathbf{x}_{c,t}^\top W_t^{-1} D_t^\top (r_t - D_t \theta^a)| > \eta s_t) \leq 2 \exp\left(-\frac{2\eta^2 s_t^2}{\|D_t W_t^{-1} \mathbf{x}_{c,t}\|^2}\right) \leq 2 \exp(-2\eta^2) = \frac{1}{T},$$

where the last inequality used the fact that

$$s_t^2 = \mathbf{x}_{c,t}^\top W_t^{-1} \mathbf{x}_{c,t} = \mathbf{x}_{c,t}^\top W_t^{-1} (I_d + D_t^\top D_t) W_t^{-1} \mathbf{x}_{c,t} \geq \mathbf{x}_{c,t}^\top W_t^{-1} D_t^\top D_t W_t^{-1} \mathbf{x}_{c,t} = (D_t W_t^{-1} \mathbf{x}_{c,t})^2.$$

Now applying a union bound, we can guarantee, with probability at least $1 - 1/T$, that for all arms $a \in \mathcal{A}$,

$$|\mathbf{x}_{c,t}^\top W_t^{-1} D_t^\top (r_t - D_t \theta^a)| \leq \eta s_t.$$

We next bound the bias term in the Equation above:

$$\|W_t^{-1} \mathbf{x}_{c,t}\| = \sqrt{\mathbf{x}_{c,t}^\top W_t^{-1} I_d W_t^{-1} \mathbf{x}_{c,t}} \leq \sqrt{\mathbf{x}_{c,t}^\top W_t^{-1} (I_d + D_t^\top D_t) W_t^{-1} \mathbf{x}_{c,t}} \leq \sqrt{\mathbf{x}_{c,t}^\top W_t^{-1} \mathbf{x}_{c,t}} = s_t.$$

This concludes the proof by showing that the total error is bounded by $(\eta + 1)s_t$ with high probability. **Q.E.D.**

Having selected the most appropriate form of the confidence radius, the proof below completes the argument in Proposition 3 of Section 3.3, providing a detailed explanation of the weighted error bound.

Proof of Proposition 3. Using the notation from the Disjoint LinUCB algorithm, and noting that the shared parameter θ_c is consistent across all nodes, we proceed as follows.

$$\begin{aligned} \mathbf{x}_{c,t}^\top \tilde{\theta}_t - \mathbf{x}_{c,t}^\top \theta &= \sum_{j=1}^N \omega_j \mathbf{x}_{c,t}^\top \tilde{\theta}_{j,t} - \sum_{j=1}^N \omega_j \mathbf{x}_{c,t}^\top \theta_j \\ &= \sum_{j=1}^N \omega_j \mathbf{x}_{c,t}^\top W_{j,t}^{-1} b_{j,t} - \sum_{j=1}^N \omega_j \mathbf{x}_{c,t}^\top W_{j,t}^{-1} (I_d + D_{j,t}^\top D_{j,t}) \theta_j \\ &= \sum_{j=1}^N \omega_j \mathbf{x}_{c,t}^\top W_{j,t}^{-1} D_{j,t}^\top r_{j,t} - \sum_{j=1}^N \omega_j \mathbf{x}_{c,t}^\top W_{j,t}^{-1} (\theta_j + D_{j,t}^\top D_{j,t} \theta_j) \\ &= \sum_{j=1}^N (\omega_j \mathbf{x}_{c,t})^\top W_{j,t}^{-1} D_{j,t}^\top (r_{j,t} - D_{j,t} \theta_j) - \sum_{j=1}^N (\omega_j \mathbf{x}_{c,t})^\top W_{j,t}^{-1} \theta_j. \end{aligned}$$

Because of $\|\theta\| \leq 1$ under Assumption 1, it follows that

$$\left| \mathbf{x}_{c,t}^\top \tilde{\theta}_t - \mathbf{x}_{c,t}^\top \theta \right| \leq \left| \sum_{j=1}^N (\omega_j \mathbf{x}_{c,t})^\top W_{j,t}^{-1} D_{j,t}^\top (r_{j,t} - D_{j,t} \theta_j) \right| + \left\| \sum_{j=1}^N (\omega_j \mathbf{x}_{c,t})^\top W_{j,t}^{-1} \theta_j \right\|.$$

This decomposition splits the prediction error into a variance term (first) and a bias term (second).

Variance term. Define the martingale difference sequence for each node j as $M_j = \omega_j \mathbf{x}_{c,t}^\top W_{j,t}^{-1} D_{j,t}^\top (r_{j,t} - D_{j,t} \theta)$. Owing to the statistical independence of samples indexed by Ψ_t , we have $E[r_{j,t} - D_{j,t} \theta_j] = \mathbb{E}[M_j] = 0$ for all nodes j . By the Cauchy-Schwarz inequality, M_j is bounded by

$$|M_j| \leq \omega_j \|D_{j,t} W_{j,t}^{-1} \mathbf{x}_{c,t}\| \cdot \|r_{j,t} - D_{j,t} \theta\|.$$

Define $s_{j,t} = \sqrt{\mathbf{x}_{c,t}^\top W_{j,t}^{-1} \mathbf{x}_{c,t}}$ for each node j . Applying Hoeffding's inequality to the variance term,

$$\begin{aligned} \Pr\left(|\mathbf{x}_{c,t}^\top W_{j,t}^{-1} D_{j,t}^\top (r_{j,t} - D_{j,t} \theta_j)| > \eta s_{j,t}\right) &\leq \exp\left(-\frac{2\eta^2 s_{j,t}^2}{\|D_{j,t} W_{j,t}^{-1} \mathbf{x}_{c,t}\|^2}\right) \\ &\leq \exp(-2\eta^2) = \left(\frac{\delta}{2T}\right)^4, \end{aligned}$$

where the first inequality follows from the fact that

$$\begin{aligned} s_{j,t}^2 &= \mathbf{x}_{c,t}^\top W_{j,t}^{-1} \mathbf{x}_{c,t} = \mathbf{x}_{c,t}^\top W_{j,t}^{-1} (I_d + D_{j,t}^\top D_{j,t}) W_{j,t}^{-1} \mathbf{x}_{c,t} \\ &\geq \mathbf{x}_{c,t}^\top W_{j,t}^{-1} D_{j,t}^\top D_{j,t} W_{j,t}^{-1} \mathbf{x}_{c,t} = (D_{j,t} W_{j,t}^{-1} \mathbf{x}_{c,t})^2. \end{aligned}$$

According to Azuma's inequality, for a martingale sequence $\{S_n\}$ with bounded increments $|S_k - S_{k-1}| \leq c_k$ implies

$$\Pr(|S_N - S_0| \geq \lambda) \leq 2 \exp\left(-\frac{\lambda^2}{2 \sum_{k=1}^N c_k^2}\right).$$

Substituting $\lambda = \eta \cdot \tilde{s}_t$ and $c_j = \omega_j \eta \cdot s_{j,t}$, we obtain

$$\sum_{j=1}^N c_j^2 = \sum_{j=1}^N (\omega_j^a)^2 \eta^2 s_{j,t}^2 = \sum_{j=1}^N (\omega_j^a)^2 \eta^2 \mathbf{x}_{c,t}^\top W_{j,t}^{-1} \mathbf{x}_{c,t} = \sum_{j=1}^N (\omega_j^a \mathbf{x}_{c,t})^\top W_{j,t}^{-1} (\omega_j^a \mathbf{x}_{c,t}).$$

Hence, the inequality $\Pr\left(\left|\sum_{j=1}^N M_j\right| > \eta \tilde{s}_t\right) \leq 2 \exp\left(-\frac{\lambda^2}{2 \sum_{k=1}^N c_k^2}\right)$ becomes

$$\begin{aligned} \Pr\left(\left|\sum_{j=1}^N M_j\right| > \eta \tilde{s}_t\right) &\leq 2 \exp\left(-\frac{\eta^2 (\tilde{s}_t)^2}{2 \sum_{j=1}^N (\omega_j^a \mathbf{x}_{c,t})^\top W_{j,t}^{-1} (\omega_j^a \mathbf{x}_{c,t})}\right) \\ &\leq 2 \exp\left(-\frac{\eta^2}{2}\right) = \frac{1}{T}. \end{aligned}$$

Applying a union bound over all arms $a \in \mathcal{A}$, we conclude that, with probability at least $1 - 1/T$,

$$\sum_{j=1}^N (\omega_j \mathbf{x}_{c,t})^\top W_{j,t}^{-1} D_{j,t}^\top (r_{j,t} - D_{j,t} \theta_j) \leq \eta \tilde{s}_t.$$

Bias term. By expanding the squared ℓ_2 -norm of the bias term, we obtain

$$\left\| \sum_{j=1}^N (\omega_j \mathbf{x}_{c,t})^\top W_{j,t}^{-1} \right\|^2 = \sum_{j=1}^N \sum_{q=1}^N (\omega_j \mathbf{x}_{c,t})^\top W_{j,t}^{-1} W_{q,t}^{-1} (\omega_q \mathbf{x}_{c,t}).$$

Define the threshold $\kappa_t := \frac{1}{1 + \max_j \lambda_{\max}(D_{j,t}^\top D_{j,t})}$. All nodes in the network \mathcal{G} are compared with the threshold. Let $\mathcal{U}_t = \{j \mid \omega_j \geq \kappa_t\}$ denote nodes with large weights, and $\mathcal{Z}_t = \{q \mid \omega_q < \kappa_t\}$ denote nodes with small weights. Define $n_1 := |\mathcal{U}_t|$ and $n_2 := |\mathcal{Z}_t|$. It follows that $n_1 + n_2 = N$. The double sum decomposes into three parts:

$$\left\| \sum_{j=1}^N (\cdot) \right\|^2 = \underbrace{\sum_{j,q \in \mathcal{U}} (\cdot)}_{\text{Term 1}} + \underbrace{\sum_{j,q \in \mathcal{Z}} (\cdot)}_{\text{Term 2}} + 2 \underbrace{\sum_{j \in \mathcal{U}, q \in \mathcal{Z}} (\cdot)}_{\text{Term 3}}.$$

For nodes j where $\omega_j \geq \kappa_t$, we apply the matrix inequality $I_d \preceq \omega_j(I_d + D_{q,t}^\top D_{q,t})$ and obtain

$$\text{Term 1} \leq \sum_{j \in \mathcal{U}} \sum_{q \in \mathcal{U}} (\omega_j \mathbf{x}_{c,t})^\top W_{j,t}^{-1} \omega_j (I_d + D_{q,t}^\top D_{q,t}) W_{q,t}^{-1} (\omega_q \mathbf{x}_{c,t}).$$

Owing to the symmetry and diagonal dominance of $(I_d + D_{q,t}^\top D_{q,t})$, we retain for Term 1 the original bound corresponding to Disjoint LinUCB,

$$\text{Term 1} \leq \sum_{j=1}^N (\omega_j \mathbf{x}_{c,t})^\top W_{j,t}^{-1} (\omega_j \mathbf{x}_{c,t}) = \tilde{s}_t^2.$$

Because $\sum_{j \in \mathcal{U}} \omega_j \leq n_1$, $\sum_{q \in \mathcal{Z}} \omega_q \leq 1 - \kappa_t n_1$, and design matrix $W_t = I + \sum_{\tau=1}^t \mathbf{x}_\tau \mathbf{x}_\tau^\top \succeq I$. For Terms 2 and 3, we establish the following key inequality:

$$\begin{aligned} |\text{Term 2} + \text{Term 3}| &\leq R^2 \left[2 \left(\sum_{j \in \mathcal{U}} \omega_j \right) \left(\sum_{\text{small } q} \omega_q \right) + \left(\sum_{q \in \mathcal{Z}} \omega_q \right)^2 \right] \\ &\leq R^2 [2(1 - \kappa_t n_1)n_1 + (1 - \kappa_t n_1)^2], \end{aligned}$$

where $R := \max_{i \in [N], t \in [T]} \|\mathbf{x}_{i,c,t}\| < \infty$.

Define $f(n_1) := 2(1 - \kappa_t n_1)n_1 + (1 - \kappa_t n_1)^2$, with domain $0 \leq n_1 \leq \lfloor \frac{1}{\kappa_t} \rfloor$, because the condition $1 - \kappa_t n_1 \geq 0$ is necessary for the existence of \mathcal{Z} .

To find the maximum of $f(n_1)$, we compute the derivative $f'(n_1) = 2(1 - \kappa_t n_1) + 2n_1(-\kappa_t) + 2(1 - \kappa_t n_1)(-\kappa_t) = 2 - 4\kappa_t n_1 - 2\kappa_t + 2\kappa_t^2 n_1$. Setting it to zero yields

$$(2\kappa_t^2 - 4\kappa_t)n_1 + (2 - 2\kappa_t) = 0 \implies n_1^* = \frac{1 - \kappa_t}{\kappa_t(2 - \kappa_t)}.$$

We know $\frac{1 - \kappa_t}{\kappa_t(2 - \kappa_t)} \leq \frac{1}{\kappa_t} \iff 1 - \kappa_t \leq 2 - \kappa_t$, so the maximum value in the domain is

$$f(n_1^*) = \frac{1}{\kappa_t(2 - \kappa_t)}.$$

Therefore, the upper bound for the latter two terms,

$$|\text{Term 2} + \text{Term 3}| \leq \frac{R^2}{\kappa_t(2 - \kappa_t)}.$$

We now consider the behavior of the cross terms (Term 2 and Term 3) over different time scales.

1. *For small t :* In the early stages, κ_t is bounded away from zero, and these two terms remain uniformly bounded as $0 \leq n_1 \leq \lfloor \frac{1}{\kappa_t} \rfloor$. Their cumulative contribution to regret from time step 1 to t is therefore bounded by $O(\log t)$, which is negligible compared to the dominant $O(\sqrt{t})$ term.

2. *For large t :* As t grows, $\lambda_{\max}(D_t^\top D_t) \rightarrow \infty$, $\kappa_t \rightarrow 0$ and all weights satisfy $\omega_j > \kappa_t$. Consequently, $n_2 \rightarrow 0$, and both Term 2 and Term 3 vanish.

Overall, the total contribution of the cross terms over all t is bounded:

$$\sum_{t=1}^T |\text{Term 2} + \text{Term 3}| = O(1),$$

which is asymptotically negligible compared to the dominant $\tilde{O}(\sqrt{T})$ regret term. Hence, the prediction error satisfies

$$\left| \mathbf{x}_{i,c,t}^\top \tilde{\theta}_{i,t}^a - \mathbf{x}_{i,c,t}^\top \theta_i^a \right| \leq (\eta + 1) \tilde{s}_t + \zeta_t,$$

where $\tilde{s}_t = \sqrt{\sum_{j=1}^N (\omega_j \mathbf{x}_{c,t})^\top W_{j,t}^{-1} (\omega_j \mathbf{x}_{c,t})}$, ζ_t collects the cross-term contributions with $\sum_{t=1}^T \zeta_t = O(1)$.

Q.E.D.

REMARK 5. The quantity $\eta = \sqrt{\log(2T)}/2$ serves as a confidence parameter that governs the tail probability in the associated concentration bound. It is derived from Hoeffding-type inequalities and ensures that the prediction error remains bounded with high probability $1 - 1/T$ over T time steps. In the NetLinUCB algorithm, the exploration parameter is set as $\alpha^{\text{ridge}} \leq 1 + \eta$, which directly controls the width of the upper confidence bound.

With the error bound established, we now derive the regret bound of the algorithm over all time steps and all nodes. The following proof completes the argument for Theorem 1 in Section 3.3.

Proof of Theorem 1. We decompose the total regret into common and node-specific component.

Common component. Based on the results established in previous propositions, we bound the cumulative regret incurred by the shared component as

$$R_1(T) = \sum_{t=1}^T r_{c,t}^{a_t^*} - \sum_{t=1}^T r_{c,t}^{a_t} \leq (1 + \eta) \sum_{i=1}^N \sum_{t=1}^T \sqrt{\sum_{j=1}^N (\omega_{ji}^{a_t} \mathbf{x}_{i,c,t})^\top (W_{j,t}^{a_t})^{-1} (\omega_{ji}^{a_t} \mathbf{x}_{i,c,t})} + (1 + \eta) \sum_{i=1}^N \sum_{t=1}^T \zeta_{i,t},$$

where $\sum_{t=1}^T \zeta_{i,t} = O(1)$ for each node i , representing the bounded contributions of bias cross-terms. Because these grow $O(\log T)$ with time, they are asymptotically negligible compared to the dominant $O(\sqrt{T})$ term and are henceforth omitted from the analysis.

For each node j , the regularized covariance matrix $W_{j,t}^k$ associated with arm $a^{(k)}$ is defined as $W_{j,t}^k = I + \sum_{\tau \in \Psi_{j,t}^k} \mathbf{x}_{j,\tau} \mathbf{x}_{j,\tau}^\top$, where $\Psi_{j,t}^k$ denotes the set of time steps up to t at which node j selected arm $a^{(k)}$, and $n_{j,t}^k = |\Psi_{j,t}^k|$ is the corresponding count.

We decompose $W_{j,t}^k$ into two parts, $W_{j,t}^k = \underbrace{I}_A + \underbrace{\sum_{\tau \in \Psi_{j,t}^k} \mathbf{x}_{j,\tau} \mathbf{x}_{j,\tau}^\top}_B$. By the eigenvalue property of positive semi-definite matrices,

$$\lambda_{\min}(A+B) \geq \lambda_{\min}(A) + \lambda_{\min}(B).$$

Given that $A = I$, we have $\lambda_{\min}(A) = 1$. In the LinUCB setting, the context vectors are bounded, i.i.d., and span the feature space, which implies that the population covariance matrix $\mathbb{E}[\mathbf{x}^\top \mathbf{x}]$ is full-rank with $\lambda_{\min} > 0$. Consequently, there exists a positive definite matrix \mathcal{V} , s.t. $\frac{1}{n_{j,t}^k} \sum_{\tau \in \Psi_{j,t}^k} \mathbf{x}_{j,\tau} \mathbf{x}_{j,\tau}^\top \succ \mathcal{V}$. Consequently, the matrix $B = \sum_{\tau \in \Psi_{j,t}^k} \mathbf{x}_{j,\tau} \mathbf{x}_{j,\tau}^\top$ satisfies $\lambda_{\min}(B) \geq n_{j,t}^k \cdot \lambda_{\min}(\mathcal{V})$. Let $c := \lambda_{\min}(\mathcal{V}) > 0$, then $\lambda_{\min}(B) \geq c \cdot n_{j,t}^k$. Hence, $\lambda_{\min}(W_{j,t}^k) \geq 1 + c \cdot n_{j,t}^k$; for any vector $\mathbf{x}_{i,c,t}$ with $\|\mathbf{x}_{i,c,t}\| \leq 1$,

$$\mathbf{x}_{i,c,t}^\top W_{j,t}^{-1} \mathbf{x}_{i,c,t} \leq \frac{\|\mathbf{x}_{i,c,t}\|^2}{\lambda_{\min}(W_{j,t}^k)} \leq \frac{d_c}{1 + c \cdot n_{j,t}^k}.$$

Let $n_t^k = \sum_{j=1}^N |\Psi_{j,t}^k|$ denote the total number of times arm k has been selected across all nodes up to time t . The weights ω_{ji}^k , which quantify the influence of node j on node i for arm k , are updated via $\omega_{ji}^k \propto \frac{n_{i,t}^k \cdot n_{j,t}^k}{(n_t^k)^2} + \frac{1}{\text{dist}(\mathbf{x}_{i,c,t}, \mathbf{x}_{j,c,t})}$ followed by symmetric normalization and smoothing to ensure $\sum_{j=1}^N \omega_{ji}^k = 1$ for each i, k . Although these weight updates ω_{ji}^k depend on both the arm-selection term and the context-similarity term, our analysis focuses on the arm-selection component because it directly impacts the exploration counts $n_{j,t}^k$ that appear in the regret bound, while the similarity-based alignment term only affects the normalization and does not alter the leading-order regret dependence.

The instantaneous regret $\Delta_{i,c,t} = r_{i,c,t}^{a_t^*} - r_{i,c,t}^{a_t}$ for node i and the selected arm $k = a_t$ is bounded as follows:

$$\begin{aligned} \Delta_{i,c,t} &\leq (1+\eta) \sqrt{\sum_{j=1}^N (\omega_{ji}^k)^2 \frac{d_c}{1+c \cdot n_{j,t}^k}} = (1+\eta) \sqrt{\sum_{j=1}^N \left(\frac{\frac{n_{i,t}^k \cdot n_{j,t}^k}{(n_t^k)^2}}{\frac{n_{i,t}^k \cdot \sum_j n_{j,t}^k}{(n_t^k)^2}} \right)^2 \frac{d_c}{1+c \cdot n_{j,t}^k}} \\ &= (1+\eta) \sqrt{\sum_{j=1}^N \left(\frac{n_{j,t}^k}{n_t^k} \right)^2 \frac{d_c}{1+c \cdot n_{j,t}^k}} \leq (1+\eta) \sqrt{\frac{d_c}{(n_t^k)^2} \sum_{j=1}^N \frac{(n_{j,t}^k)^2}{c \cdot n_{j,t}^k}} \\ &= (1+\eta) \sqrt{\frac{d_c}{c(n_t^k)^2} \sum_{j=1}^N n_{j,t}^k} = (1+\eta) \sqrt{\frac{d_c}{c(n_t^k)^2} \sum_{j=1}^N n_{j,t}^k} = (1+\eta) \sqrt{\frac{d_c}{cn_t^k}}. \end{aligned}$$

Because each regret term of the form $\sqrt{\frac{1}{n_t^k}}$ is only incurred when arm k is selected. That is, across all nodes, for each arm we accumulate the terms of $\sqrt{\frac{d_c}{cn_t^k}}$ from $n_t^k = 1$ to $n_t^k = n_T^k$, and at time step T , $\sum_{k \in \mathcal{A}} n_T^k = NT$.

Therefore, for the final regret, we rewrite the total regret in terms of arm selections,

$$R_1(T) = \sum_{i=1}^N \sum_{t=1}^T \Delta_{i,c,t} = \sum_{k \in \mathcal{A}} \sum_{m=1}^{n_T^k} (1 + \eta) \sqrt{\frac{d_c}{c \cdot m}}.$$

Applying the Cauchy–Schwarz inequality to the sum over m , we have,

$$R_1(T) = \sum_{k \in \mathcal{A}} \sum_{m=1}^{n_T^k} (1 + \eta) \sqrt{\frac{d_c}{c \cdot m}} \leq \sum_{k \in \mathcal{A}} (1 + \eta) \sqrt{n_T^k \sum_{m=1}^{n_T^k} \frac{d_c}{c \cdot m}}.$$

Using standard bandit analysis techniques and an integral approximation, we obtain

$$\sqrt{n_T^k \sum_{m=1}^{n_T^k} \frac{d_c}{c \cdot m}} \leq \sqrt{\frac{n_T^k \cdot d_c}{c} \log\left(\frac{c \cdot n_T^k}{d_c}\right)}.$$

Then summing over all arms,

$$\begin{aligned} R_1(T) &\leq 2(1 + \eta) \sum_{k \in \mathcal{A}} \sqrt{\frac{n_T^k \cdot d_c}{c} \log\left(\frac{c \cdot n_T^k}{d_c}\right)} \leq 2(1 + \eta) \sqrt{\left(\sum_{k \in \mathcal{A}} \frac{n_T^k \cdot d_c}{c}\right) \left(\sum_{k \in \mathcal{A}} \log\left(\frac{c \cdot n_T^k}{d_c}\right)\right)} \\ &\leq 2(1 + \eta) \sqrt{\frac{TNd_c}{c} [K \log\left(\frac{c}{d_c}\right) + \log((TN)^K)]} \leq 2(1 + \eta) \sqrt{\frac{TNd_c}{c} K \log\left(\frac{cTN}{d_c}\right)}, \end{aligned}$$

where K is the total number of arms in the set \mathcal{A} .

The cumulative regret for the shared component satisfies

$$R_1(T) = O\left(\sqrt{\frac{d_c TN}{c} \log\left(\frac{cTN}{d_c}\right)}\right).$$

Node-specific component. For each node i , the local estimation of the node-specific parameter $\theta_{i,s}$ is conducted independently using a standard Disjoint LinUCB model. Based on the regret analysis of Disjoint LinUCB (see Proposition 1), the cumulative regret from all node-specific components satisfies

$$R_2(T) \leq O\left(\sum_{i=1}^N d_{i,s} \sqrt{T \log T}\right).$$

This term aggregates the regret contributions from all node-specific features, and scales linearly in both the node-specific context dimension $d_{i,s}$ and the number of nodes N .

Total regret. Combining the bounds for the shared and node-specific components, we obtain the following overall regret bound:

$$R(T) = R_1(T) + R_2(T) = O\left(\sqrt{\frac{d_c TN}{c} \log\left(\frac{cTN}{d_c}\right)} + \sum_{i=1}^N d_{i,s} \sqrt{T \log T}\right),$$

where N is the number of nodes in the network; d_c and $d_{i,s}$ denote the dimensions of the common and node-specific context features for node i , respectively; and $c > 0$ is a constant that lower-bounds the minimum eigenvalue of the normalized context covariance matrix. This constant c captures the diversity of the shared contexts and is implicitly related to the common feature dimension d_c ; a larger value of c implies more effective exploration. **Q.E.D.**

Appendix E: Supporting Results for Net-SGD-UCB

This section presents the detailed theoretical analysis of the Net-SGD-UCB algorithm. We begin with the proof to a key technical lemma (Lemma 1) that provides a bound on a class of accumulated sequences. We then build upon this lemma to prove Proposition 4, which establishes an upper bound on the confidence radius used in the Net-SGD-UCB updates. This proposition explicitly characterizes how algorithmic parameters influence the cumulative uncertainty.

Proof of Lemma 1, Duchi et al. (2011), Lemma 4. Because of $A_t \geq A_{t-1}$, $\log A_t - \log A_{t-1} = \log \left(1 + \frac{a_t}{A_{t-1}}\right) \geq \left(\frac{a_t}{A_t}\right)$. Summing over time, we get $\sum_{t=2}^T \left(\frac{a_t}{A_t}\right) \leq \log A_T - \log A_1$. Adding the first term $\frac{a_1}{A_1} \leq 1$, we conclude that

$$\sum_{t=1}^T \left(\frac{a_t}{A_t}\right) \leq \log \left(\frac{A_T}{A_1}\right) + 1 \leq \log \left(1 + \frac{A_T}{A_1}\right) + 1.$$

Q.E.D.

Proof of Proposition 4. We apply exponential moving average (EMA) smoothing with parameter γ to update the gradient accumulation matrix G_t , where

$$G_t = \gamma G_{t-1} + (1 - \gamma) \text{diag}((\nabla_{\theta} \mathcal{L}_t)^{\odot 2}).$$

Accumulating along time steps, we obtain

$$G_t = (1 - \gamma) \sum_{\tau=1}^t \gamma^{t-\tau} \text{diag}((\nabla_{\theta} \mathcal{L}_{\tau})^{\odot 2}) + \gamma^{t-1} I.$$

Focusing on each diagonal entry, the h -th component is given by

$$(G_t)_{hh} = (1 - \gamma) \sum_{\tau=1}^t \gamma^{t-\tau} \left(\frac{\partial \mathcal{L}_{\tau}}{\partial \theta_h}\right)^2 + \gamma^{t-1}.$$

Because the loss function $\mathcal{L}_t(\theta)$ is the squared loss and the reward function is linear with noise ϵ and a fixed unknown parameter θ , we have

$$\frac{\partial \mathcal{L}_{\tau}}{\partial \theta_h} = -(r_{\tau} - \mathbf{x}_{\tau}^{\top} \theta)(\mathbf{x}_{\tau})_h = -\epsilon_{\tau}(\mathbf{x}_{\tau})_h,$$

where $(G_t)_{hh}$ denotes the h -th diagonal entry and $(\mathbf{x}_s)_h$ denotes the h -th component of the vector.

So $(G_t)_{hh} = (1 - \gamma) \sum_{\tau=1}^t \gamma^{t-\tau} \epsilon_{\tau}^2 (\mathbf{x}_{\tau})_h^2 + \gamma^{t-1}$.

Next, consider the sum of $\mathbf{x}_t^{\top} G^{-1} \mathbf{x}_t$ over time:

$$\begin{aligned} \sum_{t=1}^T \mathbf{x}_t^{\top} G^{-1} \mathbf{x}_t &= \sum_{t=1}^T \sum_{h=1}^d \frac{(\mathbf{x}_t)_h^2}{(G_t)_{hh}} \\ &= \sum_{h=1}^d \sum_{t=1}^T \frac{(\mathbf{x}_t)_h^2}{(1 - \gamma) \sum_{\tau=1}^t \gamma^{t-\tau} \epsilon_{\tau}^2 (\mathbf{x}_{\tau})_h^2 + \gamma^{t-1}} \end{aligned}$$

$$\begin{aligned}
&\leq \sum_{h=1}^d \sum_{t=1}^T \frac{(\mathbf{x}_t)_h^2}{(1-\gamma) \sum_{\tau=1}^t \gamma^{t-\tau} \epsilon_\tau^2(\mathbf{x}_\tau)_h^2} \\
&= \sum_{h=1}^d \sum_{t=1}^T \frac{1}{(1-\gamma) \epsilon_t^2} \cdot \frac{\epsilon_t^2(\mathbf{x}_t)_h^2}{\sum_{\tau=1}^t \gamma^{t-\tau} \epsilon_\tau^2(\mathbf{x}_\tau)_h^2} \\
&\leq \sum_{h=1}^d \sum_{t=1}^T \frac{1}{(1-\gamma)^2 \epsilon_t^2} \cdot \frac{\epsilon_t^2(\mathbf{x}_t)_h^2}{\sum_{\tau=1}^t \epsilon_\tau^2(\mathbf{x}_\tau)_h^2},
\end{aligned}$$

where $d = d_c + d_s$ is the dimension of the contexts. The last inequality holds because in our algorithm $\gamma \in [0, 1]$ is chosen close to 1 to ensure more stable parameter updates.

By applying Lemma 1, which states $\sum_{t=1}^T \left(\frac{a_t}{A_t}\right) \leq 2 \log\left(1 + \frac{A_T}{A_1}\right)$, and using the boundedness of the context \mathbf{x}_s , we obtain

$$\sum_{t=1}^T \frac{\epsilon_t^2(\mathbf{x}_t)_h^2}{\sum_{\tau=1}^t \epsilon_\tau^2(\mathbf{x}_\tau)_h^2} \leq 2 \log\left(1 + \sum_{\tau=1}^T \epsilon_\tau^2(\mathbf{x}_\tau)_h^2\right) \leq 2 \log(\sigma^2 T).$$

We then apply Jensen's inequality to handle the term, $\sum_{h=1}^d \sum_{t=1}^T \frac{1}{(1-\gamma)^2 \epsilon_t^2} \cdot \frac{\epsilon_t^2(\mathbf{x}_t)_h^2}{\sum_{\tau=1}^t \epsilon_\tau^2(\mathbf{x}_\tau)_h^2}$. Because ϵ_t is independent of \mathcal{F}_{t-1} and is a noise term with variance σ^2 , we calculate the expectation of this term to facilitate analysis of the final result. We have

$$\mathbb{E}\left[\frac{1}{\epsilon_t^2} \cdot w_t \middle| \mathcal{F}_{t-1}\right] \leq \frac{1}{\mathbb{E}[\epsilon_t^2 | \mathcal{F}_{t-1}]} \mathbb{E}[w_t | \mathcal{F}_{t-1}] = \frac{1}{\sigma^2} \mathbb{E}[w_t | \mathcal{F}_{t-1}],$$

where $w_t = \frac{\epsilon_t^2(\mathbf{x}_t)_h^2}{\sum_{\tau=1}^t \epsilon_\tau^2(\mathbf{x}_\tau)_h^2}$. Therefore, we have

$$\begin{aligned}
\mathbb{E}\left[\sum_{t=1}^T \frac{1}{(1-\gamma)^2 \epsilon_t^2} \cdot \frac{\epsilon_t^2(\mathbf{x}_t)_h^2}{\sum_{\tau=1}^t \epsilon_\tau^2(\mathbf{x}_\tau)_h^2}\right] &\leq \frac{1}{(1-\gamma)^2 \sigma^2} \mathbb{E}\left[\sum_{t=1}^T \frac{\epsilon_t^2(\mathbf{x}_t)_h^2}{\sum_{\tau=1}^t \epsilon_\tau^2(\mathbf{x}_\tau)_h^2}\right] \\
&\leq \frac{2 \log(\sigma^2 T)}{(1-\gamma)^2 \sigma^2}.
\end{aligned}$$

Summing over $h = 1, \dots, d$ yields the final result.

Next, we analyze the variance introduced by momentum update, which is

$$\begin{aligned}
v_{i,k}^{(t)} &= \mu v_{i,k}^{(t-1)} + (1-\mu) \nabla \mathcal{L}^{(t)} \\
&= (1-\mu) \sum_{\tau=1}^t \mu^{t-\tau-1} \nabla \mathcal{L}^{(\tau)}.
\end{aligned}$$

Because the arm selection and reward at each time step are independent, the expectation becomes

$$\begin{aligned}
\mathbb{E}\left[\|v_{i,k}^{(t)}\|^2\right] &= (1-\mu)^2 \mathbb{E}\left[\left\|\sum_{\tau=1}^t \mu^{t-\tau-1} \nabla \mathcal{L}^{(\tau)}\right\|^2\right] \\
&= (1-\mu)^2 \sum_{\tau=1}^t \mu^{2(t-\tau)} \mathbb{E}\left[\|\nabla \mathcal{L}^{(\tau)}\|^2\right].
\end{aligned}$$

Geometric series summation satisfies $\sum_{\tau=1}^t \mu^{2(t-\tau)} = \frac{1-\mu^{2t}}{1-\mu^2} \leq \frac{1}{1-\mu^2}$, we obtain the temporal cumulative variance bound:

$$\begin{aligned} \sum_{t=1}^T \mathbb{E} \left[\|v_{i,k}^{(t)}\|^2 \right] &\leq (1-\mu)^2 \sum_{t=1}^T \sum_{\tau=1}^t \mu^{2(t-\tau)} \mathbb{E} \left[\|\nabla \mathcal{L}^{(\tau)}\|^2 \right] \\ &= (1-\mu)^2 \sum_{\tau=1}^T \mathbb{E} \left[\|\nabla \mathcal{L}^{(\tau)}\|^2 \right] \sum_{t=\tau}^T \mu^{2(t-\tau)} \\ &\leq \frac{(1-\mu)^2}{1-\mu^2} \sum_{\tau=1}^T \mathbb{E} \left[\|\nabla \mathcal{L}^{(\tau)}\|^2 \right]. \end{aligned}$$

According to Lemma 3 of Reddi et al. (2019), the cumulative effect of momentum is upper bounded by $O(\log T)$. Then we obtain $\sum_{\tau=1}^t \mathbb{E} \left[\|\nabla \mathcal{L}^{(\tau)}\|^2 \right] \leq \sigma^2 L^2 \log T$. Thus,

$$\sum_{t=1}^T \mathbb{E} \left[\|v_{i,k}^{(t)}\|^2 \right] \leq \frac{(1-\mu)^2 \sigma^2 L^2 \log T}{1-\mu^2} = \frac{(1-\mu) \sigma^2 L^2 \log T}{1+\mu}.$$

Combining both terms, we obtain

$$\mathbf{x}_t^\top G^{-1} \mathbf{x}_t \leq \sum_{t=1}^T \frac{2d \log(\sigma^2 T)}{(1-\gamma)^2 \sigma^2} + \frac{(1-\mu) \sigma^2 \log T}{(1+\mu)(1-\gamma)},$$

where d is the dimension of the contexts, σ^2 is the variance of the noise of our reward function, μ is the momentum parameter, $\gamma \in [0, 1]$ is the smoothing parameter. **Q.E.D.**

Building upon the confidence radius bound derived in Proposition 4, we now analyze the cumulative regret incurred by the Net-SGD-UCB algorithm at each node. The complete proof of Proposition 5 is provided below.

Proof of Proposition 5. We first establish the high-probability condition required for the analysis. The algorithm maintains a global accumulation matrix G_t for each node i , which is updated using the gradients of the selected arms. For arm k at time t , the corresponding confidence interval is given by

$$\hat{\mu}_t \pm \alpha^{\text{sgd}} \sqrt{\mathbf{x}_t^{k\top} G_t^{-1} \mathbf{x}_t}.$$

We aim to ensure that this confidence bound holds with high probability. This guarantee depends on the stochastic noise in the reward observations. The noise ϵ_t in the reward propagates through the matrix G_t , introducing randomness in the estimated gradients. By controlling the cumulative effect of these noise terms over all coordinates and time steps, we ensure that the true mean reward lies within the stated confidence interval with probability at least $1 - 1/T$.

We define the normalized noise component for the h -th coordinate as

$$z_{t,h} = \frac{(\mathbf{x}_t)_h \epsilon_t}{(G_t)_{hh}},$$

where $(G_t)_{hh}$ denotes the h -th diagonal entry, and $(\mathbf{x}_s)_h$ denotes the h -th entry of the context vector. Given that $\epsilon_t \sim \text{sub-Gaussian}(\sigma^2)$ and \mathbf{x}_t is bounded, each $z_{t,h}$ is also sub-Gaussian. Applying the sub-Gaussian tail inequality, we obtain

$$\mathbf{P} \left(\left| \sum_{t=1}^T z_{t,h} \right| \geq \beta \mid \mathcal{F}_{T-1} \right) \leq 2 \exp \left(-\frac{\beta^2}{2\sigma^2} \right).$$

By choosing $\beta = \sigma \sqrt{2 \log(2dT)}$ and applying a union bound over $h = 1, \dots, d$, we conclude that with probability at least $1 - \frac{1}{T}$,

$$\left| \sum_{h=1}^d \sum_{t=1}^T \frac{(\mathbf{x}_t)_h \epsilon_t}{\sqrt{(G_t)_{hh}}} \right| \leq \sigma \sqrt{2dT \log(2dT)}.$$

This concentration result guarantees that, with high probability, the confidence interval

$$\hat{\mu}_t \pm \alpha^{\text{sgd}} \sqrt{\mathbf{x}_t^\top G_t^{-1} \mathbf{x}_t}$$

contains the true expected reward. Because the sub-Gaussian noise contribute is of the same order as the confidence radius. Here, the exploration parameter α^{sgd} is chosen such that it scales with $1 + \sigma^2$, thereby ensuring that the noise-induced deviation is absorbed into the radius and the bound remains valid.

We now turn to the regret analysis. Under the above high-probability event, the instantaneous regret incurred from selecting suboptimal arm k_t instead of the optimal arm k^* is bounded by

$$\Delta_t \leq 2\alpha^{\text{sgd}} \sqrt{\mathbf{x}_t^{k_t \top} G_t^{-1} \mathbf{x}_t^{k_t}}.$$

Summing over time and applying the Cauchy–Schwarz inequality, we get

$$R(T) \leq 2\alpha^{\text{sgd}} \sqrt{T \sum_{t=1}^T \mathbf{x}_t^\top G^{-1} \mathbf{x}_t}.$$

From Proposition 4, we know

$$\sum_{t=1}^T \mathbf{x}_t^\top G^{-1} \mathbf{x}_t \leq \frac{2d \log(\sigma^2 T)}{(1-\gamma)^2 \sigma^2} + \frac{(1-\mu)\sigma^2 \log T}{(1+\mu)(1-\gamma)}.$$

Substituting this bound into the regret expression yields the final bound:

$$R(T) \leq 2\alpha^{\text{sgd}} \left(\frac{\sqrt{2dT \log(\sigma^2 T)}}{(1-\gamma)\sigma} + \sigma \sqrt{\frac{(1-\mu)T \log T}{(1+\mu)(1-\gamma)}} \right),$$

where d is the dimension of the contexts, σ^2 is the variance of the noise in the reward function, μ is the momentum parameter, and γ is the smoothing parameter. **Q.E.D.**

After establishing the regret bound for each individual node, we now extend the analysis to the entire network by incorporating the weighted influence among nodes through the inter-node weight matrix. We provide the full proof of Theorem 2 in Section 3.4 below.

Proof of Theorem 2. We decompose the cumulative regret into two parts: the contribution from the shared parameter, denoted $R_1(T)$, and the node-specific regret, denoted $R_2(T)$.

When a suboptimal arm a_t is selected, the regret arising from the shared parameter $\theta_c^{a_t}$ is analyzed in four steps: decomposition of the estimation error, control of the variance, bias analysis, and evaluation of the weighted confidence bound.

Each node i maintains an estimate $\hat{\theta}_{c,i}^{a_t} \in \mathbb{R}^{d_c}$ of the true shared parameter $\theta_c^{a_t}$, and defines the estimation error as $\Delta_{i,c,t} = \hat{\theta}_{c,i}^{a_t} - \theta_c^{a_t}$. At each time step t , node i updates its estimate by aggregating its neighbors' estimates and performing a stochastic gradient step, which is

$$\hat{\theta}_{c,i,t}^{a_t} = \sum_{j=1}^N \omega_{ji}^{a_t} \hat{\theta}_{c,j,t-1}^{a_t} + \eta^{\text{sgd}} \nabla \mathcal{L}_{i,t}.$$

Subtracting $\theta_c^{a_t}$ yields the recursive form of the estimation error:

$$\Delta_{i,c,t} = \sum_{j=1}^N \omega_{ji}^{a_t} \Delta_{j,c,t-1} + \eta^{\text{sgd}} \nabla \mathcal{L}_{i,t}.$$

This recursion separates the aggregation dynamics from the stochastic gradient error. Decomposing the error gives

$$\Delta_{i,c,t} = \underbrace{(\Delta_{i,c,t} - \mathbb{E}[\Delta_{i,c,t}])}_{\text{Variance}} + \underbrace{(\mathbb{E}[\Delta_{i,c,t}] - \theta_c^{a_t})}_{\text{Bias}}.$$

Variance term. By applying EMA smoothing with factor γ , and following results from decentralized SGD (Lian et al. 2017), the variance term is bound as $O(\frac{\sigma^2}{(1-\gamma)m})$, where m denotes the number of SGD updates. Combining this with global updates and arm selection structure, we obtain the bound

$$\mathbb{E} [\|\Delta_{i,c,t} - \mathbb{E}[\Delta_{i,c,t}]\|^2] \leq \frac{\sigma^2}{(1-\gamma)n_t^k},$$

where σ^2 is the noise variance and n_t^k denotes selected counts before time t among all nodes for arm k .

Because updates are only triggered when arm k is selected, we split the sum accordingly. Following the same analytical approach as in NetLinUCB, we aggregate over all time steps and nodes:

$$\begin{aligned} \sum_{i=1}^N \sum_{t=1}^T \frac{\sigma^2}{(1-\gamma)n_t^k} &\leq \sum_{k \in \mathcal{A}} \sum_{m=1}^{n_T^k} \frac{\sigma^2}{(1-\gamma)m} \leq \sum_{k \in \mathcal{A}} \frac{1-\gamma}{\sigma^2} \log\left(\frac{\sigma^2}{(1-\gamma)n_T^k}\right) \\ &\leq \frac{1-\gamma}{\sigma^2} \cdot K \log\left(\frac{\sigma^2}{(1-\gamma) \sum_{k \in \mathcal{A}} n_T^k}\right) = \frac{(1-\gamma)K}{\sigma^2} \log\left(\frac{\sigma^2}{(1-\gamma)NT}\right), \end{aligned}$$

which becomes negligible as $T \rightarrow \infty$.

Bias term. Because all nodes share the same true parameter $\theta_c^{a_t}$, the expected estimation bias vanishes:

$$\sum_{t=1}^T \|\mathbb{E}[\Delta_{i,c,t}] - \theta_c^{a_t}\|^2 \leq C^2 T \max_j \|\theta_c^{a_t} - \theta_{c,j}^*\|^2 = 0,$$

where $C = \mathcal{O}(1)$ is a bounded constant.

Confidence radius term. As T increases, both the variance and bias components become negligible. We now focus on bounding the contribution from the weighted confidence radius. The regret contribution becomes

$$\sum_{i=1}^N \sum_{t=1}^T \sqrt{\sum_{j=1}^n (\omega_{ji})^2 \mathbf{x}_{c,t}^\top G_{c,t}^{-1} \mathbf{x}_{c,t}}.$$

According to Proposition 4, $\sum_{t=1}^T \mathbf{x}_t^\top G_t^{-1} \mathbf{x}_t \leq \frac{\sqrt{2d_{i,s} \log(\sigma^2 T)}}{(1-\gamma)\sigma} + \sigma \sqrt{\frac{(1-\mu) \log T}{(1+\mu)(1-\gamma)}}$, and noting that the dominant component in ω_{ji} primarily arises from arm selection statistics,

$$\sum_{i=1}^N \sum_{t=1}^T \sqrt{\sum_{j=1}^n (\omega_{ji})^2 \mathbf{x}_{i,c,t}^\top G_{j,c,t}^{-1} \mathbf{x}_{i,c,t}} = \sum_{i=1}^N \sum_{t=1}^T \sqrt{\sum_{j=1}^n \left(\frac{n_{j,t}^k}{n_t^k}\right)^2 \mathbf{x}_{i,c,t}^\top G_{j,c,t}^{-1} \mathbf{x}_{i,c,t}}.$$

Final bound for shared component R_1 . Applying the Cauchy–Schwarz inequality, we derive

$$\begin{aligned} \sum_{t=1}^T \sum_{i=1}^N r_{i,c,t} &\leq \sqrt{NT \cdot \sum_{t=1}^T \sum_{i=1}^N \sum_{j=1}^n \left(\frac{n_{j,t}^k}{n_t^k}\right)^2 \mathbf{x}_{i,c,t}^\top G_{j,c,t}^{-1} \mathbf{x}_{i,c,t}} \\ &= \sqrt{NT \cdot \sum_{t=1}^T \sum_{j=1}^n \left(\frac{n_{j,t}^k}{n_t^k}\right)^2 \left(\sum_{i=1}^N \mathbf{x}_{i,c,t}\right)^\top G_{j,c,t}^{-1} \left(\sum_{i=1}^N \mathbf{x}_{i,c,t}\right)} \\ &\leq \sqrt{NT \cdot \sum_{t=1}^T \left(\sum_{i=1}^N \mathbf{x}_{i,c,t}\right)^\top G_{j,c,t}^{-1} \left(\sum_{i=1}^N \mathbf{x}_{i,c,t}\right)} \\ &= \mathcal{O}\left(\frac{\sqrt{Nd_c T \log(\sigma^2 T)}}{1-\gamma}\right), \end{aligned}$$

where the weighting factor satisfies $\sum_{j=1}^n \left(\frac{n_{j,t}^k}{n_t^k}\right)^2 \leq \frac{(\sum_{j=1}^n n_{j,t}^k) \cdot (\sum_{j=1}^n n_{j,t}^k)}{(n_t^k)^2} = 1$. The final inequality holds because each matrix $G_{j,c,t}$ aggregates information from all nodes through the corresponding context vectors $\sum_{i=1}^N \mathbf{x}_{i,c,t}$. Thus, the bound from Proposition 4 applies. The residual contributions from inner products involving shared contexts are absorbed into the analysis of the node-specific component $R_2(T)$.

Final bound for node-specific component R_2 . We now bound the regret arising from node-specific parameters, corresponding to N independent instances of SGD-UCB. Using the regret bound from Proposition 5, each node contributes

$$\mathcal{O}\left(\frac{\sqrt{2d_{i,s} T \log(\sigma^2 T)}}{(1-\gamma)\sigma} + \sigma \sqrt{\frac{(1-\mu) T \log T}{(1+\mu)(1-\gamma)}}\right).$$

Summing over all nodes yields

$$R_2(T) = O\left(\sum_{i=1}^N \frac{\sqrt{2d_{i,s}T \log(\sigma^2 T)}}{(1-\gamma)\sigma} + N\sigma \sqrt{\frac{(1-\mu)T \log T}{(1+\mu)(1-\gamma)}}\right).$$

This completes the proof by combining both the shared and node-specific regret components.

Q.E.D.

Appendix F: Supplementary Numerical Experiment Results

We present detailed results for additional simulation instances in Figures 7 and 8. These experiments, conducted with a total of $N = 12$ cities, complement the analysis in the main text (Section 5) and explore a range of challenging conditions. Specifically, we vary: (i) the proportion of shared versus local context dimensions, (ii) the variance of the context distribution, (iii) the number of arms, and (iv) the reward gap between the optimal and second-best actions. Each setting emphasizes different aspects of model generalization and exploration efficiency, and different algorithms exhibit varying levels of performance depending on the contextual structure and reward pattern.



Figure 6 Numerical legend. In all figures below, blue and orange denote Disjoint and Shared LinUCB, respectively. Red and green curves represent NetLinUCB and Net-SGD-UCB under varying simulation environment settings. Each label denotes a sub-network structure: **(3*4)** and **(6*2)** correspond to 3 or 2 fully connected sub-networks with 4 or 6 nodes each, respectively, while **(12)** denotes a single fully connected network. In Net-based models, information is shared within each sub-network but not across sub-networks. Disjoint LinUCB corresponds to the degenerate case **(1*12)** with no sharing, and Shared LinUCB to the extreme case **(12)** with full sharing.

Table 3 quantifies the impact of network structure on uncertainty reduction. NetLinUCB achieves up to a 95% decrease in confidence radius under fully connected settings, highlighting the benefits of structured parameter aggregation. In contrast, Net-SGD-UCB maintains consistent reductions across all connectivity levels, reflecting its robustness through adaptive variance tracking. This distinction underscores the complementary strengths of the two methods: NetLinUCB improves significantly with denser graphs, while Net-SGD-UCB performs reliably under both sparse and dense settings.

We further analyze the evolution of confidence intervals produced by different algorithms. As shown in Figure 9, all methods gradually converge toward the true revenue curve. Disjoint LinUCB exhibits slower convergence due to its independent learning per node. Shared LinUCB and NetLinUCB demonstrate faster reduction in uncertainty by exploiting cross-node parameter sharing.

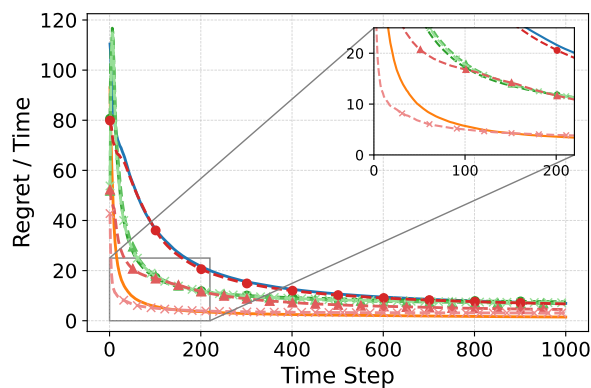


Figure 6 (a) Low shared-to-specific context ratio, $(t, \frac{R(t)}{t})$

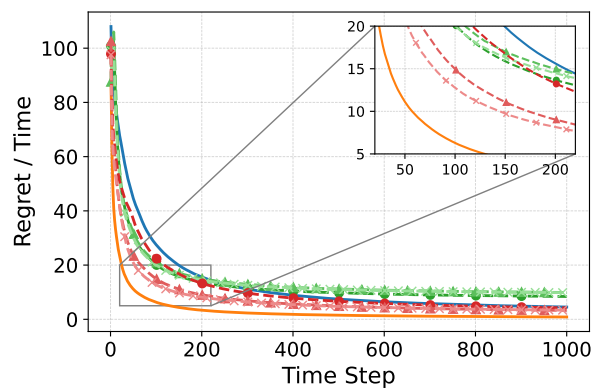


Figure 6 (b) High shared-to-specific context ratio, $(t, \frac{R(t)}{t})$

Figure 7 Performance under different shared-to-specific context ratios. When shared context dominates, Shared LinUCB outperforms others by leveraging transferable structure; in contrast, when local context dominates, NetLinUCB converges faster, and Disjoint LinUCB becomes more competitive due to its independence.

Method	3×4	6×2	12
Net-SGD-UCB	21.72%	22.40%	22.66%
NetLinUCB	39.97%	84.75%	94.82%

Table 3 Confidence interval reduction ratio compared to Disjoint LinUCB, under different network connectivity.

Notably, Net-SGD-UCB begins with wider intervals due to its adaptive gradient-based updates, but achieves consistent narrowing over time, thanks to its EMA-based variance control. This highlights the trade-off between stability and adaptivity in decentralized high-dimensional environments.

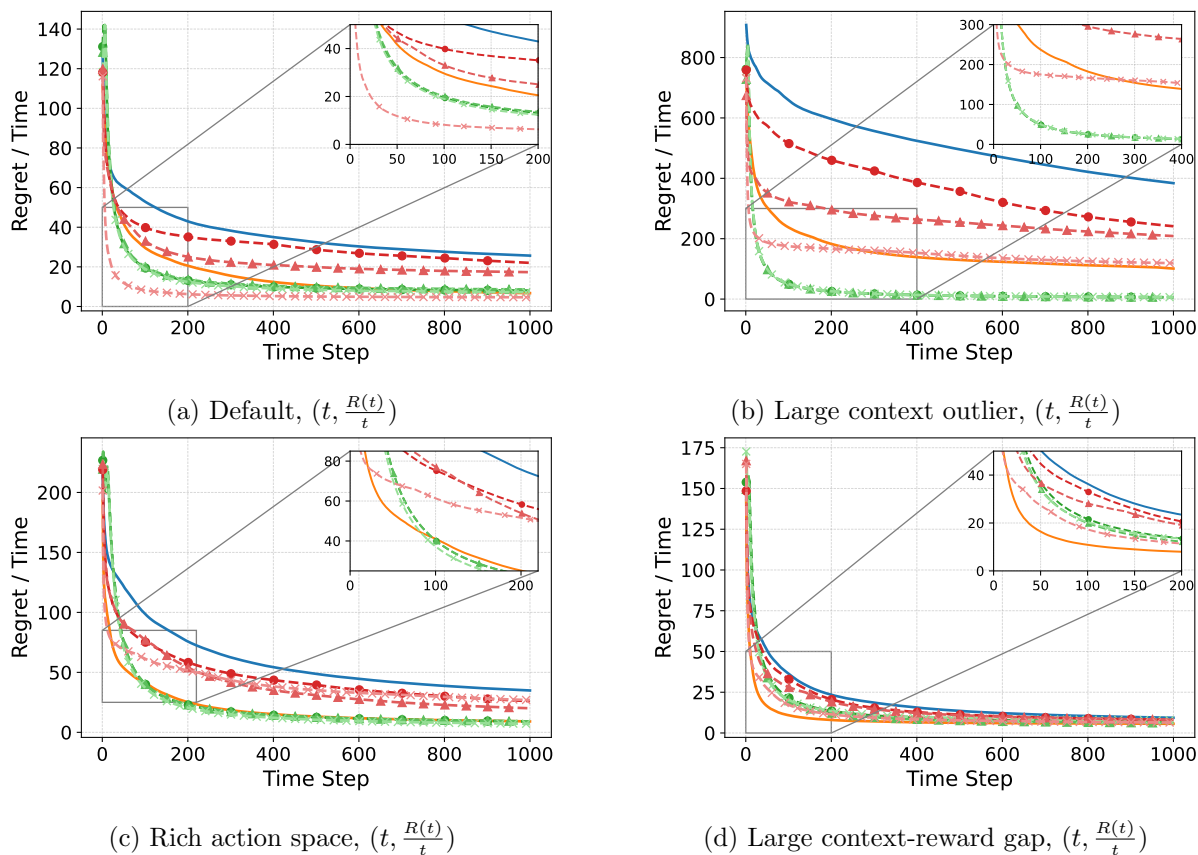


Figure 8 Performance across challenging scenarios. (a) shows the default configuration, serving as a baseline for comparison with the following three cases. (b) introduces a large contextual outlier, where Net-SGD-UCB remains robust due to adaptive variance tracking. (c) increases the number of actions, under which Net-SGD-UCB performs best by efficiently scaling with arm space. (d) features a large reward gap, where Shared LinUCB achieves the lowest regret by rapidly distinguishing optimal arms through aggressive generalization. In contrast, NetLinUCB performs best under the small reward gap in (a), benefiting from fine-grained estimation via network-based inference.

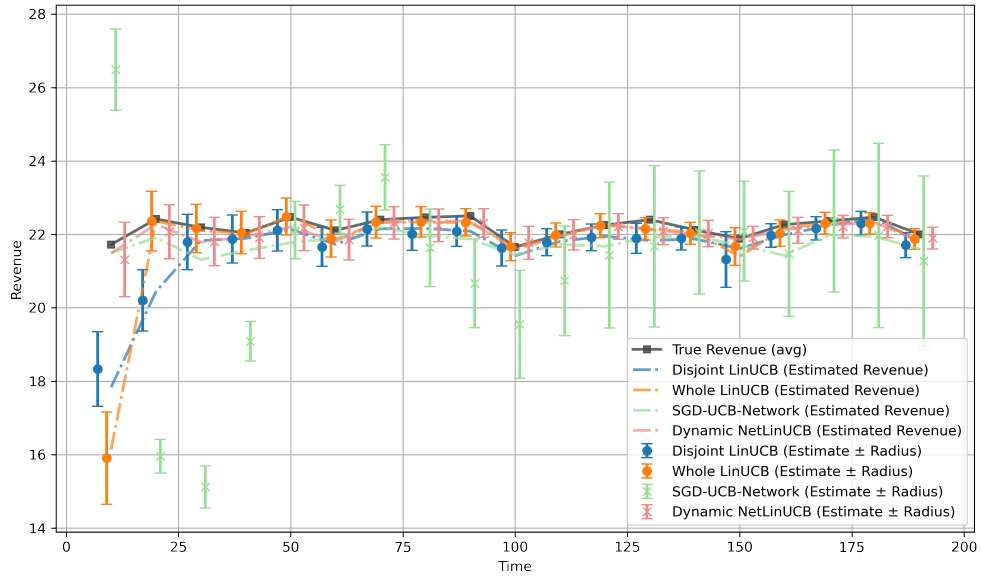


Figure 9 True revenue curve and estimated confidence intervals across all cities under different algorithms.